

Opto-Electronic Advances

ISSN 2096-4579

CN 51-1781/TN

Table-top optical parametric chirped pulse amplifiers: past and present

Audrius Dubietis and Aidas Matijošius

Citation: Dubietis A, Matijošius A. Table-top optical parametric chirped pulse amplifiers: past and present. *Opto-Electron Adv*, 6, 220046(2023).

<https://doi.org/10.29026/oea.2023.220046>

Received: 3 March 2022; Accepted: 12 May 2022; Published online: 30 September 2022

Related articles

Compact pulsed thulium-doped fiber laser for topographical patterning of hydrogels

Elizabeth Lee, Biao Sun, Jiaqi Luo, Satnam Singh, Deepak Choudhury, Derrick Yong, Xia Yu, Qijie Wang

Opto-Electronic Advances 2020 3, 190039 doi: [10.29026/oea.2020.190039](https://doi.org/10.29026/oea.2020.190039)

Observation and optimization of 2 μm mode-locked pulses in all-fiber net anomalous dispersion laser cavity

Wanzhuo Ma, Desheng Zhao, Runmin Liu, Tianshu Wang, Quan Yuan, Hao Xiong, Haiying Ji, Huilin Jiang

Opto-Electronic Advances 2020 3, 200001 doi: [10.29026/oea.2020.200001](https://doi.org/10.29026/oea.2020.200001)

More related article in Opto-Electron Journals Group website 

 Opto-Electronic
Advances

<http://www.ojournal.org/oea>



 OE_Journal



 @OptoElectronAdv

DOI: [10.29026/oea.2023.220046](https://doi.org/10.29026/oea.2023.220046)

Table-top optical parametric chirped pulse amplifiers: past and present

Audrius Dubietis^{†*} and Aidas Matijošius[†]

The generation of power- and wavelength-scalable few optical cycle pulses remains one of the major challenges in modern laser physics. Over the past decade, the development of table-top optical parametric chirped pulse amplification-based systems was progressing at amazing speed, demonstrating excellent performance characteristics in terms of pulse duration, energy, peak power and repetition rate, which place them at the front line of modern ultrafast laser technology. At present, table-top optical parametric chirped pulse amplifiers comprise a unique class of ultrafast light sources, which currently amplify octave-spanning spectra and produce carrier-envelope phase-stable, few optical cycle pulses with multi-gigawatt to multi-terawatt peak powers and multi-watt average powers, with carrier wavelengths spanning a considerable range of the optical spectrum. This article gives an overview on the state of the art of table-top optical parametric chirped pulse amplifiers, addressing their relevant scientific and technological aspects, and provides a short outlook of practical applications in the growing field of ultrafast science.

Keywords: optical parametric amplification; post-compression; ultrafast nonlinear optics; high harmonic generation

Dubietis A, Matijošius A. Table-top optical parametric chirped pulse amplifiers: past and present. *Opto-Electron Adv* 6, 220046 (2023).

Introduction

A tremendous progress in ultrafast solid-state laser technology was inspired by the invention of chirped pulse amplification (CPA) technique by D. Strickland and G. Mourou in 1985¹, facilitating rapid development of laser-related experimental sciences and opening new areas of physics, technology and multidisciplinary research², and whose significance was certified by the award of the Nobel Prize in Physics in 2018. The idea of the CPA technique is to boost the energy of an ultrashort pulse, while avoiding very high fluence and intensity in the laser amplifier, which incurs detrimental nonlinear effects, such as self-focusing and self-phase-modulation (accumulation of the nonlinear phase) that distort spatial and temporal characteristics of the laser pulse and eventually

lead to optical damage of the amplifying medium, optical elements and coatings. This is accomplished by temporal stretching (chirping) the short input pulse without the loss of its spectral content in an optical setup that introduces certain group delay dispersion. Then the long chirped pulse is amplified in a laser amplifier, and thereafter recompressed to its original duration in a setup which introduces exactly opposite group delay dispersion, thus producing an ultrashort pulse with high peak power at the output. At present, the CPA technique constitutes the standard conceptual basis of modern ultrafast solid-state lasers and laser systems, making high peak-power ultrashort pulses routinely available.

Introduction of the optical parametric chirped pulse amplification (OPCPA) concept, in which the laser

Laser Research Center, Vilnius University, Saulėtekio Avenue 10, LT-10223 Vilnius, Lithuania.

[†]These authors contributed equally to this work.

*Correspondence: A Dubietis, E-mail: audrius.dubietis@ff.vu.lt

Received: 3 March 2022; Accepted: 12 May 2022; Published online: 30 September 2022



Open Access This article is licensed under a Creative Commons Attribution 4.0 International License.

To view a copy of this license, visit <http://creativecommons.org/licenses/by/4.0/>.

© The Author(s) 2023. Published by Institute of Optics and Electronics, Chinese Academy of Sciences.

amplifier was replaced by the optical parametric amplifier³, paved a new avenue in the development of ultrafast all solid-state laser sources. OPCPA favorably combines the advantages of CPA with the advantages of optical parametric amplification, which offers very high gain, low thermal effects, great wavelength flexibility and intrinsically broad amplification bandwidth, extending well beyond that afforded by existing solid-state laser amplifiers. Over the past two decades, the OPCPA incorporated the advanced techniques of ultrafast optical parametric amplification^{4–6}, becoming a mature and robust amplification technology that is applied to a very broad class of ultrafast light sources ranging from compact table-top^{7–12} to facility-size systems¹³. Table-top OPCPA systems represent a unique class of robust high energy and high peak power ultrafast light sources, providing optical pulses as short as few-optical cycles, with carrier wavelengths spanning a considerable part of the optical spectrum. In particular, significant efforts were dedicated to develop few optical cycle OPCPA systems operating in the mid-infrared spectral region, which is hardly accessible with currently existing ultrafast solid-state lasers and laser amplifiers, or by any other means, see e.g. ref.¹⁴. At present OPCPA is deservedly regarded as a corner stone of the emerging third-generation femtosecond technology, which foresees generation of few optical cycle pulses with high (terawatt-scale) peak powers and high (kilowatt-scale) average powers achieved simultaneously, alongside full control over the generated light waves within very broad spectral range¹⁵.

This review article gives a short historical retrospect and provides a comprehensive account on the state of the art of table-top OPCPA systems, addressing their basic components, design concepts, key features and performance in the near-infrared (NIR, around 0.8 μm), short-wave infrared (SWIR, in the 1.5–3 μm range) and mid-infrared (MIR, beyond 3 μm) spectral regions. The closing sections are dedicated to highlight some interesting developments of OPCPA, especially regarding the application of OPCPA technique to all-fiber systems, and to present a condensed overview of OPCPA applications in ultrafast laser-matter interactions, extreme nonlinear optics and high field physics.

OPCPA from time perspective

A possibility to amplify phase-modulated (chirped) pulses in the optical parametric amplifier was first con-

sidered in the mid-80's. These early theoretical and experimental works were summarized in a review article¹⁶, outlining several relevant findings concerning important aspects of optical parametric amplification, which are widely exploited in modern ultrafast optical parametric amplifiers and OPCPA systems, in particular. Firstly, it was found that the optical parametric amplifier may provide very broad gain (or phase-matching) bandwidth, extending well beyond the bandwidths required to amplify picosecond pulses, which were routinely available at that time. Secondly, it was demonstrated that the optical parametric amplifier is able to amplify chirped signal pulses without distortions of their phase characteristics. This finding in fact seeded the idea of OPCPA. Thirdly, due to phase conjugation between the signal and idler waves, amplification of chirped signal pulse results in the chirp reversal of the idler pulse, which is a by-product of the optical parametric amplification process. This last feature is currently used in modern-day OPCPA systems for chirp manipulation, allowing to greatly simplify pulse stretching and compression apparatus.

The first experimental demonstration of optical parametric chirped pulse amplification dates back to 1992³. A broadband seed was produced by spectral broadening of 1.7 ps, 1055 nm pulse from passively mode-locked Nd:glass oscillator in a single-mode fiber, which at the same time played the role of pulse stretcher due to fiber dispersion. The chirped seed pulse was amplified in a single-pass degenerate beta-barium borate crystal-based optical parametric amplifier, which was pumped by 8-ps second harmonic pulse from Nd:glass regenerative amplifier, see Fig. 1. The amplified chirped pulse was compressed to a transform limit in a grating-pair compressor, yielding 70 fs pulse with energy of 65 μJ , corresponding to a peak power of 0.9 GW at the output. Although this result looks very modest from the viewpoint of present state of the art, the authors foresaw a great potential of this technique for delivery of femtosecond pulses with terawatt (TW) peak powers by the use of large pulse stretching/compression factors employing nanosecond Q-switched lasers as energetic pump sources. Indeed, in the following years this idea was further theoretically elaborated by Ross and coworkers, who suggested several practical designs of optical parametric chirped pulse amplifiers for potentially delivering ultrashort light pulses with petawatt (PW)¹⁷ or even multi-petawatt¹⁸ peak powers and coined the generally accepted acronym "OPCPA".

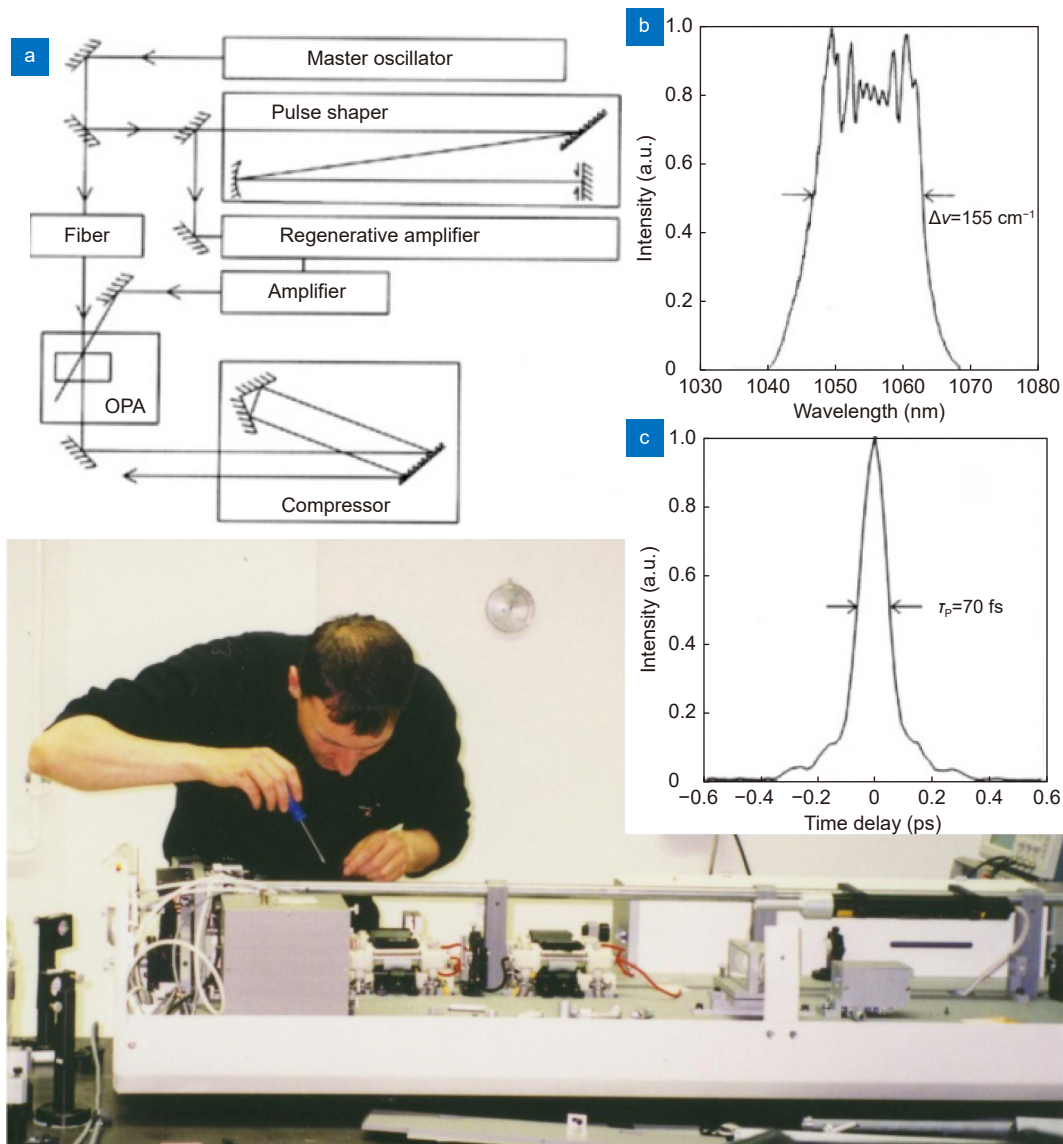


Fig. 1 | The first OPCPA. (a) Experimental setup. (b) Amplified spectrum. (c) Autocorrelation function of compressed pulse. Image at the bottom shows one of the authors (AD) aligning picosecond Nd:glass laser, which was used for driving the OPCPA experiment. Figure reproduced with permission from: (a–c) ref.³, Elsevier.

Since the beginning of current millennium, the experimental realizations of OPCPA were primarily focused on amplification of femtosecond pulses in the spectral region around $0.8 \mu\text{m}$ that is particularly important regarding the development of large-scale petawatt-class laser systems. To this end, the first experimental OPCPA setups produced pulses with TW¹⁹ and multi-TW²⁰ peak powers and compressed pulsewidths of a few hundreds of femtoseconds. Since then, the power of the output pulses has increased tremendously: from a few hundreds of TW in 2006²¹, to sub-PW in 2007²², PW in 2015²³ and multi-PW in 2017²⁴, placing these OPCPA systems alongside the most powerful petawatt-class Ti:sapphire and Nd:glass CPA laser systems. New developments are

underway, e.g. a petawatt facility fully based on OPCPA concept, Vulcan OPPEL, an all-OPCPA auxiliary PW beamline project, which will be coupled with the existing hybrid-CPA/OPCPA VULCAN laser system based on Nd:glass amplifiers²⁵.

In the early stage of these developments, smaller-scale OPCPA systems were deemed as attractive alternatives to existing Ti:sapphire laser amplifiers, serving as front-ends for high power OPCPA systems²⁶. Shortly after, amplification of very short pulses with stable carrier envelope phase (CEP), i.e. fixed phase offset between the carrier and the envelope of the pulse, was demonstrated^{27,28}, prompting the inception of compact, stand-alone OPCPA systems.

Building blocks of table-top OPCPA

Front-end

The generation of few optical cycle pulses demands production of ultrabroadband, octave-spanning spectra. These are readily provided by ultrafast Ti:sapphire oscillators^{29,30}, which are ideally suited for direct seeding of NIR OPCPA. However, other well-developed laser oscillators, such as Yb:KGW, Yb-fiber, Er-fiber, etc., produce relatively long, ~100 fs and even sub-ps (Yb:YAG) pulses, hence the generation of broadband seed requires additional spectral broadening of the pulse involving nonlinear effects. Supercontinuum generation in photonic crystal fibers³¹ suggests the most straightforward route in achieving this goal, however, imposing limitations on the pulse energy and temporal coherence. Supercontinuum generation in bulk solid-state materials³² as well as spectral broadening in noble-gas-filled hollow core fibers³³, produces fully compressible ultrabroadband pulses with much higher spectral energy density, however, both approaches require oscillator pulses to be pre-amplified to achieve sufficient pulse energy to induce nonlinear effects. Supplementary optical parametric amplifiers (OPA) and difference frequency generation (DFG) between either frequency-shifted oscillator outputs or spectral components of the ultrabroadband oscillator pulse itself (the so-called intrapulse DFG) are employed to produce broadband seed at a desired wavelength, especially concerning SWIR and MIR spectral regions, where direct generation of broadband pulses is difficult due to scarcity of suitable laser sources. Moreover, DFG using pump pulses originating from the same laser source produces broadband seed with intrinsically stable CEP³⁴, which is an important requisite of few optical cycle pulses. Eventually, high energy seed pulses are produced by more complex front-ends that use a combination of the above techniques.

Pump lasers

The repetition rate of the pump laser is of particular importance, since it sets the repetition rate of the entire OPCPA system. As high-energy pump lasers usually operate in sub-ps to 100s-ps and even ns regime, the pump pulse duration defines stretching factor of the seed pulse, and hence the dispersion management and overall arrangement of pulse stretching and compression setup. Differently from CPA, where pulse stretching in time (chirping) is performed in order to reduce the intensity

in the amplifier, in the case of OPCPA in addition it allows matching duration of the chirped seed and pump pulses. ns and 100s-ps pump pulses enable amplification to very high energies and are used to pump TW-class table-top OPCPA systems, while millijoule OPCPA outputs can be achieved with 1–10 ps pump pulses. Short (a few ps) pump pulses offer inherently high temporal contrast to amplified compressed pulses, since the optical parametric amplification process provides gain only within the time window of the pump pulse. On the other hand, such a short pulse configuration is more sensitive to the synchronization accuracy of the seed and pump pulses. A number of pump lasers were developed for OPCPA pumping, employing amplifiers based on Nd-doped laser crystals: Nd:YAG^{35–37}, Nd:YLF³⁸, Nd:YVO₄^{39,40}, hybrid setups that use Nd:YVO₄ and Nd:YAG amplifiers^{41,42}, and even a combination of Yb and Nd amplifying media^{43,44}. The diode-pumped solid state laser (DPSSL) technology, which replaced flashlamps with laser diode modules, made these pump lasers more efficient, compact and capable of operating at kHz repetition rates. The rise of Yb laser technology enabled generation of high-energy femtosecond and picosecond pulses at very high repetition rates ranging from 100s of kHz to a few MHz with excellent beam quality, beam pointing and energy stability, thus making feasible construction of high average power OPCPA systems. To this end, Yb:KGW^{45,46}, Yb:YAG⁴⁷, Yb-fiber⁴⁸ master oscillator-power amplifier systems and high power Yb:YAG amplifiers exploiting bulk^{49,50}, thin-disc⁵¹ and Innoslab configurations^{52,53} were developed as integrable parts of OPCPA setups. Finally, novel Ho:YAG⁵⁴ and Ho:YLF^{55–57} regenerative amplifiers delivering intense multi-millijoule picosecond pulses at kHz repetition rates with center wavelengths around 2 μm were developed for pumping ultrafast OPA and OPCPA systems operating at wavelengths beyond 4 μm.

Nonlinear crystals

The heart of OPCPA system is the optical parametric amplifier, which is based on nonlinear crystals with suitable optical properties. Borate crystals: beta-barium borate (BaB₂O₄, BBO), lithium triborate (LiB₃O₅, LBO), bismuth triborate (BiB₃O₆, BIBO) and recently introduced yttrium calcium oxyborate (YCa₄O(BO₃)₃, YCOB) serve as indispensable amplifying media featuring ultrabroad phase-matching bandwidths in the NIR as pumped by second harmonics of Ti:sapphire, Nd and Yb lasers^{58–60},

as well as in the SWIR under fundamental harmonic pumping of these lasers. Oxide crystals: potassium titanyl arsenate (KTiOAsO₄, KTA), potassium titanyl phosphate (KTiOPO₄, KTP), potassium niobate (KNbO₃), lithium niobate (LiNbO₃, LN) as well as its periodically poled version (PPLN) and periodically poled stoichiometric lithium tantalate (LiTaO₃, PPSLT) provide sufficient phase matching bandwidths under fundamental harmonic pumping that support amplification of few optical cycle pulses in the 1.5–4 μm wavelength range⁶¹. Non-oxide semiconductor crystals, such as gallium selenide (GaSe), silver gallium selenide (AgGaSe₂, AGSe), and especially zinc germanium phosphide (ZnGeP₂, ZGP) show excellent performance in the MIR with ~2 μm pumping from Ho lasers^{62,63}. Novel langasite oxide crystals, e.g. LGN (La₃Ga_{5.5}Nb_{0.5}O₁₄), exhibit extended transparency range, high damage threshold, superior phase-matching characteristics and large aperture size, having potential for building TW-class MIR OPCPA systems⁶⁴, while a large family of novel non-oxide Li-based materials, such as lithium thiogallate (LiGaS₂, LGS), emerge as promising materials for OPCPA in

the long-wave infrared (LWIR) region⁶⁵.

OPCPA throughout the optical spectrum

Figure 2 illustrates the current state of the art of table-top OPCPA systems in terms of output pulsewidth and central wavelength. For the sake of straightforward comparison of pulsewidths at various spectral regions, the pulse duration is expressed in multiple of optical cycles, $\tau_{oc} = \lambda_0/c$, where λ_0 is the central (carrier) wavelength and c is the speed of light in a vacuum. The color coding that indicates the usage of nonlinear crystals is instructive regarding wavelength range of their performance in providing phase-matching bandwidths that support generation of few optical cycle pulses under real experimental settings. Finally, pulse post-compression techniques based on spectral broadening in either gaseous or solid-state materials, are employed to further reduce the duration of amplified pulses. In particular, post-compression schemes are very efficient in the MIR, where direct production of pulses shorter than 4 optical cycles is still a very challenging task due to limited phase-matching bandwidths of available nonlinear crystals. Moreover, in

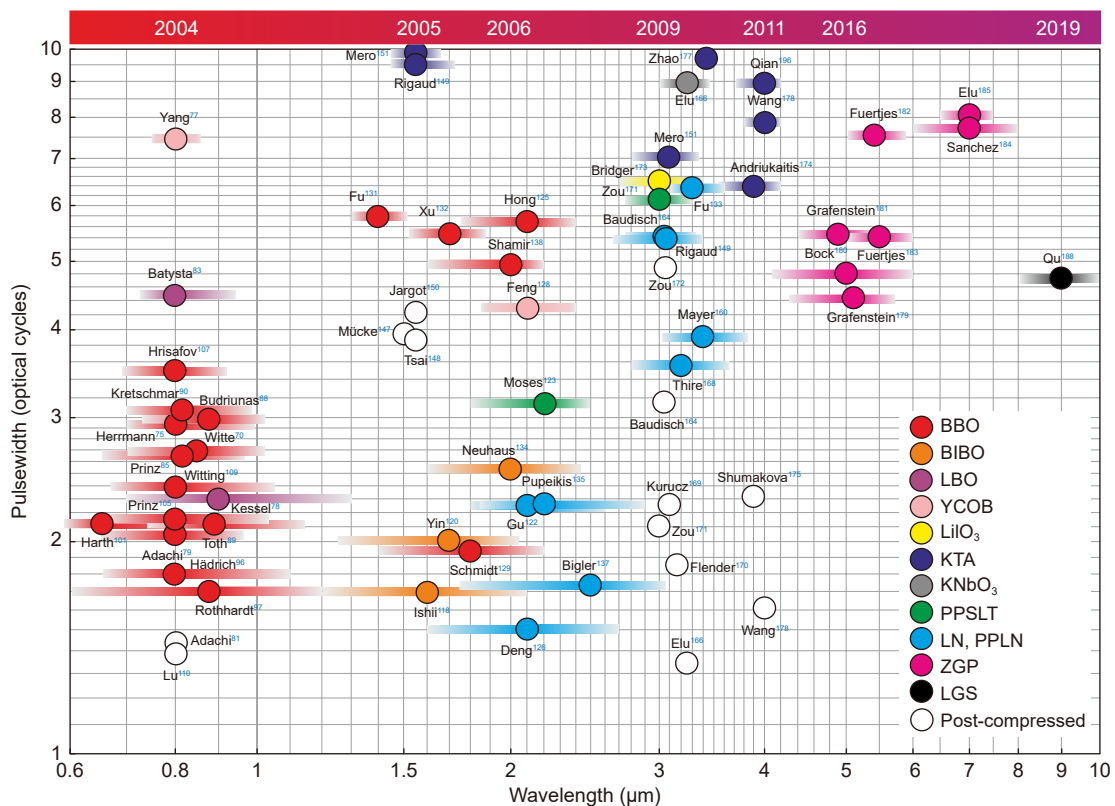


Fig. 2 | State of the art of few optical cycle table-top OPCPA systems. The central wavelength is indicated by colored circles, where color coding denotes the nonlinear crystal used as an amplifying medium. The amplified bandwidths are schematically depicted by horizontal bars, which represent the full width of the amplified spectrum. The time bar on the top marks the year of experimental inception of OPCPA in the particular wavelength region.

this spectral range both spectral broadening and temporal compression could be accomplished within a single piece of solid-state material due to favorable interplay between self-phase modulation and anomalous group velocity dispersion, offering the advantages of technical simplicity and high energy throughput of post-compression setup.

Table-top OPCPA systems comprise robust technological solutions for pump-seed synchronization and exploit a variety of pulse stretching and compression configurations, from lossy and complicated “traditional” grating-pair-based setups to simple, compact and efficient schemes based on bulk materials, made possible via dispersion management and adaptive control of pulse chirp by the use of acousto-optic programmable dispersion filters (AOPDF) and spatial light modulators (SLM). Eventually, performance of the optical parametric amplification stages is improved by engineering of phase-mismatch, pulse and beam profiles, etc. Although every particular OPCPA system is specific in its technical implementation and performance, there are general design concepts (seed production techniques, pump lasers, nonlinear crystals, amplification geometries, pulse stretching and compression setups, etc.), which share common principles for the OPCPA systems operating within a certain spectral region. In that regard, the OPCPA systems are divided into the following groups: NIR (around 0.8 μm) OPCPA, SWIR (1.5–3 μm) OPCPA, with a distinct group of OPCPA at around 1.5 μm , MIR OPCPA in the 3–4 μm range and MIR OPCPA beyond 4 μm .

OPCPA in the near infrared

The well-established architecture of NIR OPCPA systems operating around 800 nm relies on a combination of ultrafast Ti:sapphire oscillators serving as front-ends and either Nd- or Yb-doped laser amplifiers delivering energetic pump pulses via second harmonic generation. Optical parametric amplification is performed in non-collinear geometry, setting a certain crossing angle between the seed and pump beams that ensures the broadest phase matching bandwidth; a configuration that is often termed non-collinear OPCPA (NOPCPA). BBO crystal serves as indispensable and hence most widely-used amplifying medium in the NIR, providing an octave-spanning phase-matching bandwidth, which favorably matches the spectral bandwidth of the seed.

The early table-top NIR OPCPA systems were designed on the basis of Ti:sapphire oscillators optically

and/or electronically synchronized with high energy, low repetition rate (10–30 Hz) flashlamp-pumped Nd:YAG amplifiers. These NIR OPCPA systems produced few optical cycle pulses with sub-10 fs durations and multi-millijoule^{66–71} to hundreds-of-millijoule^{72–75} energies that correspond to terawatt and multi-terawatt peak powers, respectively. Out of these, the OPCPA system that produced 130 mJ, 7.7 fs pulses holds a still unbeaten record peak power of 16.7 TW among TW-class table-top OPCPA systems⁷⁵. More recently, a number of TW-class table-top OPCPA systems were demonstrated employing non-collinear broadband amplification in $\text{K}_3\text{B}_6\text{O}_{10}\text{Br}$ (KBOB)⁷⁶, YCOB⁷⁷ and LBO⁷⁸; the latter OPCPA system employed low repetition rate (10 Hz) Yb:YAG amplifier and produced 6.9 fs, 42 mJ pulses with a peak power of 5 TW.

In the pursuit of attaining high peak and high average power simultaneously, CEP-stable, 5.5 fs pulses with 2.7 mJ energy at 1 kHz repetition rate were first reported from OPCPA system based on sole Ti:sapphire laser technology, using second harmonic pump pulses from Ti:sapphire amplifier chain operating in the picosecond regime^{79,80}. An extra spectral broadening of the output pulses was performed by self-phase modulation in a thin argon jet, and post-compression to below 1.5 optical cycles (3.8 fs) was achieved in a combined chirped mirror and wedge pair compressor⁸¹. More recent developments of kHz table-top TW-class OPCPA systems strongly benefited from the advent of diode-pumped Nd- and Yb-doped laser amplifiers. To this end, 11.3 mJ, 12.1 fs pulses at 1 kHz repetition rate with an average power of 11.3 W were reported from Yb:YAG thin-disk regenerative amplifier-pumped BBO and LBO OPCPA system, which was designed as a front end at ELI-beamline facility^{82,83}. More recently, the system was upgraded to produce 15 fs, 30 mJ pulses at central wavelength of 820 nm with 30 W average power⁸⁴. Another Yb:YAG thin-disk amplifier-pumped OPCPA system based on BBO delivered high intensity contrast 7.2 fs pulses with an energy of more than 1.8 mJ at 6 kHz repetition rate; these parameters correspond to a peak power of 160 GW and an average output power exceeding 10.8 W⁸⁵.

A conceptually different front-end consisting of femtosecond Yb:KGW master oscillator-power amplifier-driven broadband OPA^{86,87} was implemented with diode-pumped Nd:YAG amplifiers running at 1 kHz repetition rate, allowing straightforward optical pump-seed synchronization, see Fig. 3. Such OPCPA system

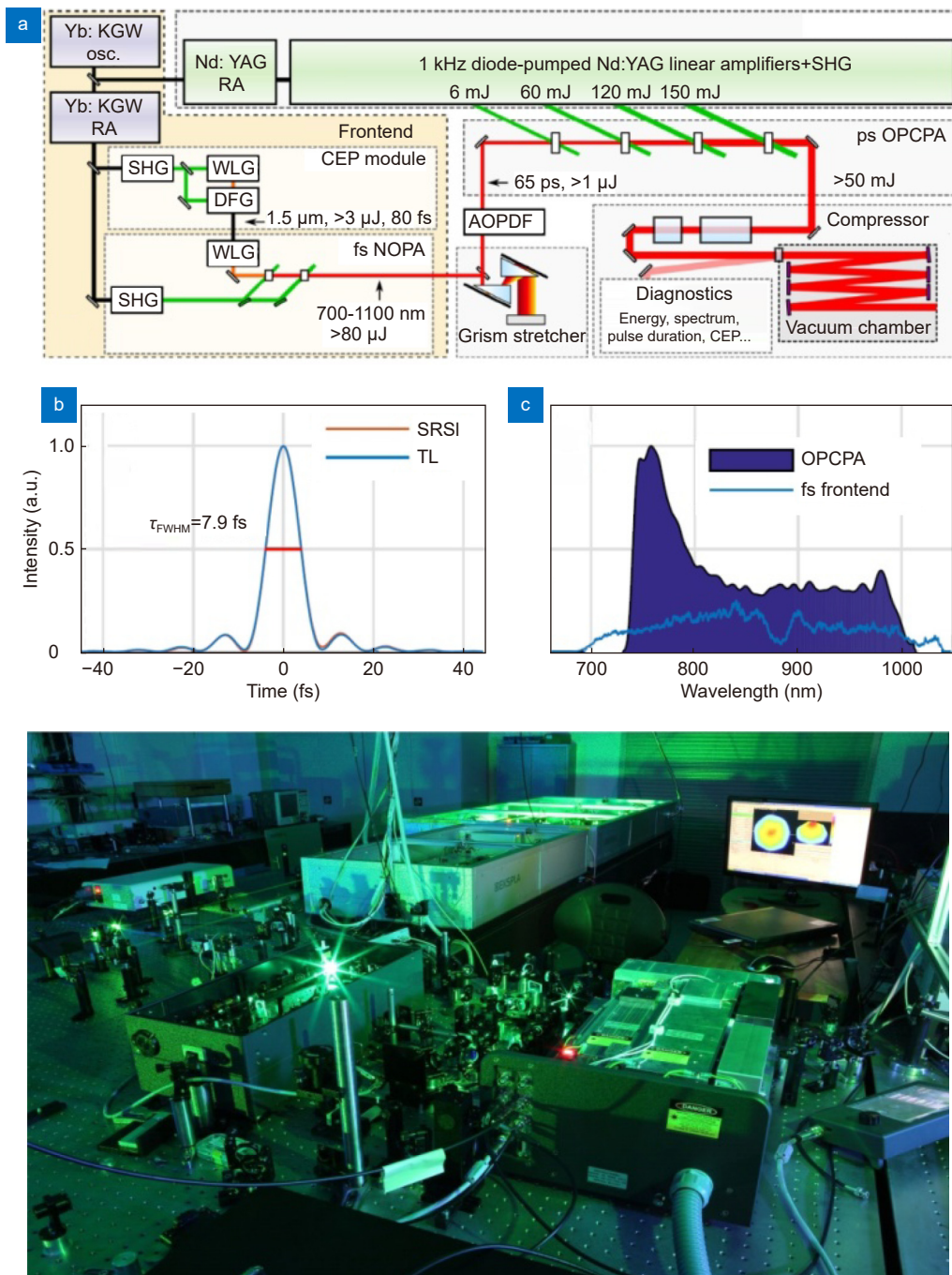


Fig. 3 | (a) Layout of multi-terawatt high average power NIR OPCPA system with complex Yb:KGW laser-based front-end, which includes supercontinuum generation, DFG and complimentary noncollinear OPA. (b) Compressed pulse envelope measured with a self-referenced spectral interferometry (SRSI) and theoretical transform-limited pulse envelope (TL). (c) Comparison of seed and amplified pulse spectra. Photo at the bottom: laboratory view of a running system. Image courtesy dr. A. Varanavičius, Laser Research Center, Vilnius University. Figure reproduced with permission from: (a–c) ref.⁸⁸, The Optical Society.

produced CEP-stable 8.8 fs, 5.5 TW pulses at a center wavelength of 880 nm with > 53 W average power⁸⁸, representing the highest figure among CEP-stabilized, multi-TW, few optical cycle OPCPA systems to date. That OPCPA system served as a prototype of the multi-TW SYLOS laser installed in 2019 at ELI-ALPS facility in

Szeged (Hungary), which is dedicated to the generation, research and application of attosecond light pulses⁸⁹. More recently, a similar Yb:KGW laser-based front-end was combined with Yb:YAG thin-disk amplifiers, producing CEP-stable 8.3 fs, 4.4 TW pulses at a center wavelength of 810 nm and 100 Hz repetition rate⁹⁰. [Figure 4](#)

summarizes the performance of multi-millijoule >100-GW and TW-class OPCPA systems operating in the NIR, which is compared to performances of OPCPA systems in the SWIR and MIR, which will be discussed in more detail in the following sections of the paper.

An interesting, wavelength-tunable (in the 680–960 nm range) OPCPA system producing 30–100 fs pulses with sub-mJ energies at 1 kHz repetition rate was developed using DPSS Nd:YVO₄ regenerative amplifier as a pump source. The system employed a complex front-end, where pulses from picosecond Yb: fiber laser were spectrally broadened in optical fiber, parametrically amplified, compressed to femtosecond duration and then used to generate supercontinuum signal which thereafter was amplified in a femtosecond broadband non-collinear OPA⁹¹.

The inception of high repetition rate NIR OPCPA systems relied upon replacement of low repetition pump lasers by high repetition rate pump sources based on Yb-fiber CPA systems^{92–96}, eventually demonstrating the 1 MHz OPCPA that produced CEP-stable pulses as short as 1.7 optical cycles (5.0 fs) with 22 W average power⁹⁷.

Substitution of Yb-fiber lasers by Yb-doped thin-disc amplifiers allowed to achieve excellent performance characteristics at repetition rates up to 500 kHz in very compact setups^{98,99}. Application of two-color (second and third harmonics) pumping concept to sequentially amplify the long- and short-wavelength portions of the seed in separate parametric amplification stages¹⁰⁰ succeeded in amplification of an ultrabroad spectrum from 450 nm to 1.3 μm, which supported a Fourier limited pulse duration of sub-3 fs, corresponding to a nearly single optical cycle¹⁰¹. The inner part of the spectrum centered at 650 nm was compressed down to 4.6 fs with energy of 1 μJ at 200 kHz repetition rate. A compact cost-efficient few optical cycle OPCPA scheme was designed on the basis of optically synchronized Ti:sapphire oscillator and CPA-free, diode-pumped Nd:YVO₄ amplifier operating at a 100 kHz repetition rate, providing seed and pump pulses, respectively¹⁰². Ultra-stable OPCPA systems producing pulse durations as short as ~6 fs and energies of ~10 μJ at 200 kHz^{103,104}, and sub-6 fs pulses with more than 50 μJ energy and 15 W of average power at 300 kHz repetition rate^{105,106} were developed

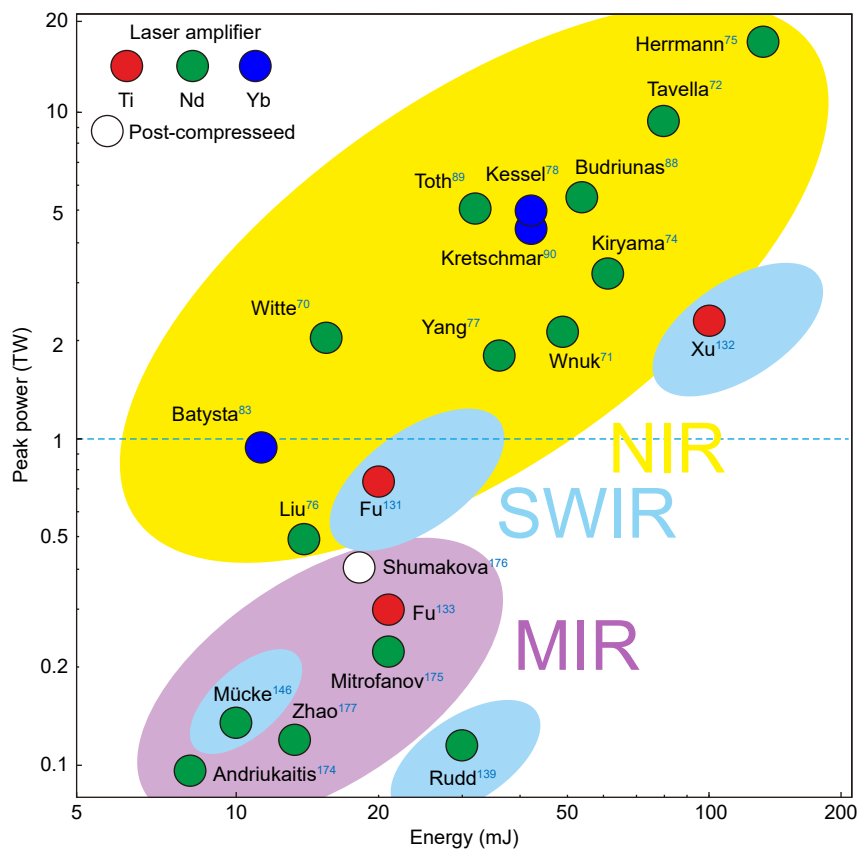


Fig. 4 | Graphical summary of the performance of multi-millijoule >100-GW and TW-class table-top OPCPA systems in the NIR (yellow area), SWIR (blue area) and MIR (magenta area). Color coding of the data points denotes the gain medium of pump laser, which is indicated in the legend.

using rod-type and thin-disc Yb:YAG laser amplifiers, respectively. Scaling of both, peak and average powers was demonstrated with 100 kHz OPCPA systems delivering few optical cycle pulses with >20 GW peak powers and average powers of 22.5 W¹⁰⁷ and 24 W^{108,109}. The output pulses from the latter OPCPA system were further spectrally broadened by nonlinear propagation in a series of thin quartz plates and subsequently compressed from 7 fs to 3.7 fs (1.5 optical cycles) by a combination of thin fused silica wedges and chirped mirrors¹¹⁰. Scaling of the average power was demonstrated with few cycle OPCPA pumped by Yb:YAG Innoslab burst amplifier with an intra-burst repetition rate of 27.5 kHz¹¹¹ and more recently, with a three-stage 1.5 kW Yb:YAG Innoslab booster amplifier operating at 10 Hz repetition rate and delivering 720–900 nm tunable, 30 fs pulses in 100 kHz bursts with an average power of 112 W¹¹². The performance of high average power NIR OPCPA systems is summarized in Fig. 5, which combines the data from both, TW-class and high repetition rate OPCPA systems.

A particularly interesting development route of high average power OPCPA systems is based on sole Yb-doped laser technology. These OPCPA systems are seeded with a broadband signal produced by bulk-generated supercontinuum instead of Ti:sapphire oscillator, and their main advantage is compactness due to simple synchronization between pump and seed pulses. To this end, sub-20 fs pulses with 16.5 W average power at 500 kHz repetition rate were produced by OPCPA system

that employed amplified femtosecond Yb-fiber laser-generated supercontinuum as a front-end and high-power picosecond Yb:YAG amplifier¹¹³. A conceptually similar OPCPA system was developed on the basis of customized commercial Yb lasers, delivering sub-20 fs pulses with energy of 0.88 mJ at 100 kHz repetition rate and constituting an average power 88.6 W¹¹⁴, which is the highest average power among NIR OPCPA systems reported so far. Even more simple and compact OPCPA schemes were elaborated on the basis of a single picosecond Yb laser source, but challenges remain to generate stable and fully compressible supercontinuum seed from picosecond pulses. To this end, a compact, wavelength-tunable between 700 and 900 nm OPCPA fully based on 1-ps Yb:YAG Innoslab amplifier was designed to provide sub-30 fs pulses with 11.4 W average power at a 3.25 MHz repetition rate¹¹⁵ (not shown in Fig. 5 to keep convenient aspect ratio of the plot) and several conceptually similar OPCPA setups operating at low (1 kHz) repetition rates were demonstrated as well^{116,117}.

OPCPA in the short-wave infrared

In contrast to NIR OPCPA, SWIR (1.5–3 μm) OPCPA systems use more energetically efficient pumping scheme, since they employ pump pulses at fundamental harmonic of the driving laser. Broadband optical parametric amplification is performed around the degeneracy wavelengths ($\sim 1.6 \mu\text{m}$ for Ti:Sapphire, $\sim 2 \mu\text{m}$ for Nd and Yb laser pumping) in various nonlinear crystals:

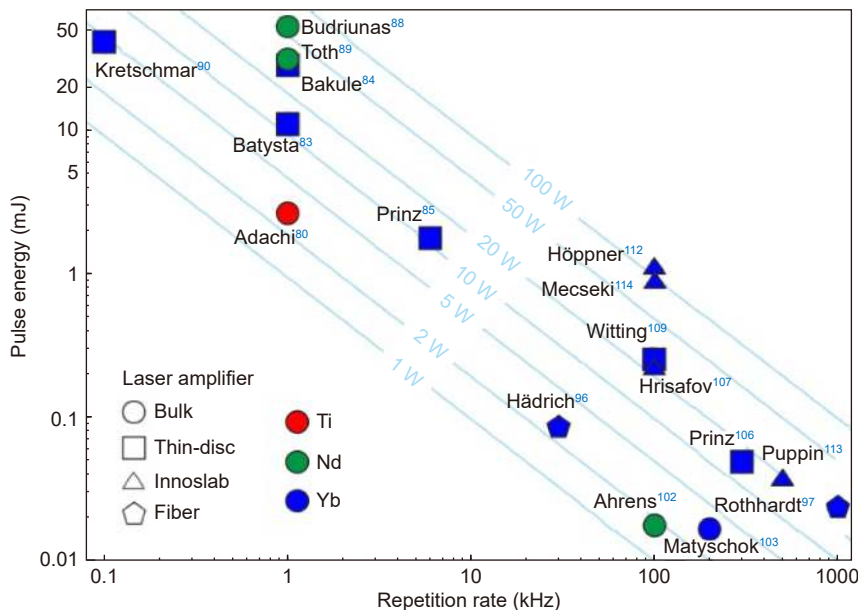


Fig. 5 | Graphical summary of the performance of high average power NIR OPCPA systems. Color coding of data points denotes the gain medium of pump laser, while different shapes indicate the configuration of laser amplifier.

BBO, BIBO, YCOB, bulk and periodically poled LN and PPSLT. The vast majority of SWIR OPCPA systems are developed around ultrafast Ti:sapphire oscillators, and the broadband seed at the required wavelength is produced by DFG, which also provides intrinsic stabilization of CEP. More complex front-ends, especially those based on Yb oscillators, involve supplementary OPA, supercontinuum generation and DFG.

Diverse SWIR OPCPA systems that produce CEP-stable few optical cycle pulses with sub-millijoule to a few millijoule energies at kHz repetition rates were developed on the basis of Ti:sapphire oscillators coupled with picosecond Ti:sapphire^{118,119}, Nd:YLF^{120–123}, Yb:YAG^{124–126} and Nd:YAG¹²⁷ amplifiers. The shortest pulses to date of 9 fs (1.7 optical cycle) at 1.6 μm ^{118,119} and 11.4 fs (2 optical cycles) at 1.7 μm ¹²⁰ were demonstrated from Ti:sapphire-pumped OPCPA based on BIBO and 10.5 fs (1.5 optical cycle) at 2.1 μm from Yb:YAG-pumped OPCPA based on MgO:PPLN¹²⁶ nonlinear crystals. More recently, a high average power OPCPA system at 2.1 μm using a commercial 500 W Yb:YAG thin disk laser as a single source for pump and seed generation was reported¹²⁸. The OPCPA system employed BIBO and YCOB crystals, producing 30 fs, 2.7 mJ pulses at 10 kHz repetition rate, setting a record average output power of 27 W in this particular wavelength interval.

Several interesting amplification concepts were proposed to simplify the OPCPA design and improve performance characteristics, especially for what concerns scaling of the peak power. In that regard, the amplification in frequency domain rather than in time domain, termed frequency domain optical parametric amplification, was introduced and experimentally demonstrated with Ti:sapphire-pumped BBO OPCPA system, yielding CEP-stable, two optical cycle (11.7 fs), 1.43 mJ pulses at 1.8 μm ¹²⁹. The idea is to independently amplify frequency components of a broadband pulse in the Fourier plane, thus avoiding spectral and spatial distortions, circumventing the limitations of gain narrowing arising from phase mismatch and damage threshold of the nonlinear crystal without the need of pulse stretching and compression setups. Another concept, dual-chirped optical parametric amplification (DC-OPA), suggested using both chirped pump and signal pulses, hence making possible to apply high-energy pump pulses and achieve large energy conversion factors without the onset of optical damage of the nonlinear crystal¹³⁰. High potential of DC-OPA was proven by applying this technique to pro-

duce few optical cycle pulses with peak powers of 0.74 TW (27 fs, 20 mJ) at 1.4 μm ¹³¹ and 2.3 TW (31 fs, 100 mJ) at 1.7 μm ¹³² in BBO-based OPCPA setups that employed a joule-class 10 Hz Ti:Sapphire laser system as a pump source, as well as achieving 0.3 TW (70 fs, 21 mJ) pulses at 3.3 μm in bulk LN crystal-based MIR OPCPA¹³³, all of which representing the highest peak powers reported so far in the SWIR and MIR spectral ranges, respectively, see Fig 4.

High (100 kHz) repetition rate SWIR OPCPA systems providing CEP-stable few optical cycle pulses with multi-GW peak powers are pumped with high average power Yb:YAG Innoslab amplifiers, while the broadband seed is produced by successive noncollinear optical parametric amplification and DFG stages driven by amplified Yb:YAG laser¹³⁴ and Ti:sapphire oscillator pulses^{135–137}. To this end, 17 fs (2.7 optical cycle) pulses at 2 μm with 10 W average power were demonstrated from BIBO-based OPCPA¹³⁴, where the authors also compared the performance characteristics of BIBO, BBO and LBO crystals, demonstrating that BIBO offers the best compromise between output power and overall stability. 16.5 fs pulses (2.2 optical cycles) at 2.2 μm with 25 W average power¹³⁵ and 14.4 fs (1.7 cycles) at 2.5 μm with 12.6 W average power¹³⁶ were reported from MgO:PPLN crystal-based OPCPA systems. A custom designed, BBO crystal-based SWIR OPCPA system employed Yb-fiber chirped pulse amplifier as a pump source and produced wavelength tunable (1.4–2.1 μm) pulses with 6 W average power as measured at 1.93 μm ¹³⁸. Figure 6 summarizes the performance of high average power SWIR OPCPA systems also including OPCPA systems operating around 1.5 μm , which are discussed below.

OPCPA around 1.5 μm

OPCPA systems with center wavelengths of around 1.5 μm comprise a rather specific group of SWIR OPCPA. Large fraction of these SWIR OPCPA systems use KTA crystal as an amplifying medium, since it exhibits a relatively broad amplification bandwidth around 1.5 μm , high transparency for the idler wave, which lies in the MIR (above 3 μm), high optical damage threshold and shows no optical degradation at high peak intensities, so promising scaling to high energies and high average powers. Indeed, although these systems produce relatively long pulses, they deliver either multi-millijoule or very high average power outputs. Moreover, several 1.5 μm OPCPA systems offer dual-wavelength operation, by

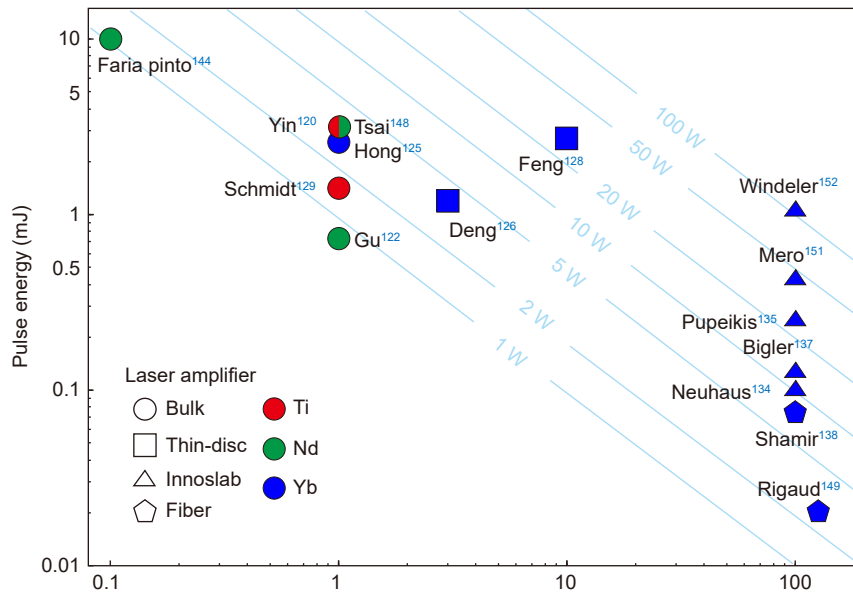


Fig. 6 | Graphical summary of the performance of high average power SWIR OPCPA systems. Color coding of data points denotes the gain medium of pump laser, while different shapes indicate the configuration of laser amplifier.

compressing both, SWIR signal and MIR idler pulses, falling into category of MIR OPCPA.

The early setups were based on femtosecond Er:fiber^{139–141} and Cr:forsterite^{142,143} oscillators serving as front-ends, electronically synchronized with Nd-laser amplifiers and produced >100 fs pulses. Out of these, a notable OPCPA system delivering 260 fs, 30 mJ pulses at 1.55 μm was demonstrated¹³⁹; a remarkable result in terms of energy even from the present day view. Recently, multi-millijoule OPCPA system of a similar architecture, but using more advanced Er-fiber front-end with a fast response piezo-mounted cavity mirror, which was used to synchronize its repetition frequency to that of Nd:YVO₄ master oscillator that seeded diode-pumped Nd:YAG amplifier, was developed to produce 220 fs, 10.5 mJ pulses with 1550 nm center wavelength at 100 Hz repetition rate¹⁴⁴. A distinctive OPCPA system was designed using front-end based on amplified Yb:KGW laser-pumped OPA, delivering passively CEP-stabilized pulses at 1.5 μm ¹⁴⁵ and optically synchronized with low repetition rate (20 Hz) Nd:YAG amplifier serving as a pump source. The OPCPA delivered 74 fs pulses with 10 mJ energy¹⁴⁶, and 2.2 mJ fraction was additionally compressed to 19.8 fs by filamentation in a noble gas cell¹⁴⁷. More recently, a similar seed generation concept was employed in KTP-based OPCPA system that was pumped by Nd:YAG amplifier at 1 kHz repetition rate. The sub-mJ fraction of CEP-stable 3 mJ, 80 fs output pulse at 1.55 μm was thereafter spectrally broadened by

passing through 9 pieces of thin quartz plates and compressed down to 20 fs duration (3.9 optical cycles) by a Fourier pulse shaper¹⁴⁸.

A robust high repetition rate dual-wavelength OPCPA system was designed on the basis of a single industrial-grade 125 kHz Yb-doped fiber femtosecond source that simultaneously provided supercontinuum seed and pump for three amplification stages based on MgO:PPLN crystal, delivering 49 fs, 20 μJ signal pulses at 1550 nm and 72 fs and 10 μJ idler pulses at 3070 nm, which were independently compressed in bulk fused silica and silicon, respectively¹⁴⁹. Thereafter this system was upgraded by replacing MgO:PPLN by KTA in the final amplification stage, and post-compressing the signal pulse at 1550 nm down to 22 fs in a multipass cell containing fused silica plate¹⁵⁰. High average power dual-beam 100 kHz KTA-based OPCPA system that employed two-branch Yb:fiber laser, DFG-based front-end and Yb:YAG amplifier as a pump source, simultaneously delivered passively CEP-stabilized 51 fs signal pulses at 1.55 μm and 73 fs idler pulses at 3.1 μm with average powers of 43 W and 12.5 W, respectively¹⁵¹. Finally, an exceptional KTA-based OPCPA system with Yb:fiber laser-pumped OPA front-end and 100 kHz repetition rate, kW-level Innoslab Yb:YAG amplifier was designed to produce ~100 fs pulses with unprecedented average power of 106.2 W at a center wavelength of 1.75 μm (see Fig. 6), also yielding continuous wavelength tunability from 1.5 to 2.0 μm ¹⁵².

Mid-infrared OPCPA

MIR is the wavelength range that is truly “no man’s land” for existing ultrafast laser sources, so MIR OPCPA systems constitute a very special class of few optical cycle sources devoted to various applications in spectroscopy, ultrafast nonlinear optics, strong-field physics and attosecond science, with a particular emphasis on high harmonic generation, whose high frequency cut-off energy scales proportionally to square of the driving wavelength. Since the very nature of optical parametric amplification process treats the signal and idler waves as fully interchangeable, this feature is widely exploited in MIR OPCPA systems, which are seeded either with SWIR signal, extracting MIR idler pulse, or directly with broadband pulse at the idler wavelength that is produced by DFG. Bulk and periodically poled LN, KTA serve as the main nonlinear crystals in the 3–4 μm wavelength range, while fine performance from PPSLT, KNbO_3 and lithium iodate (LiIO_3) was reported as well.

The inception of MIR OPCPA systems relied on the availability of compact commercial laser sources: femtosecond dual-wavelength Er: fiber master oscillator-power amplifier system and electronically synchronized diode-pumped picosecond 100 kHz Nd:YVO₄ laser¹⁵³. The broadband MIR seed pulses were produced by DFG between the two-color outputs of fiber laser, stretched in a sapphire rod, amplified in a double-stage optical parametric amplifier based on MgO:PPLN crystals and compressed by either prism or grating pair compressor, delivering ~ 1 μJ , sub-100 fs (~ 9 optical cycle) pulses with respective central wavelengths of 3.5 μm ¹⁵⁴ and 3.2 μm ¹⁵⁵. A further development of these two conceptually very similar OPCPA systems serves as an excellent example illustrating the evolution of scientific and technological ideas beyond the MIR OPCPA.

The first OPCPA system¹⁵⁴ was upgraded by using aperiodically poled MgO:PPLN crystals, providing ultrabroadband gain in a collinear amplification geometry¹⁵⁶, changing the seeding concept (from DFG to directly using the Er: fiber oscillator pulse) and employing bulk compressor¹⁵⁷. Thereafter the system was redesigned to broaden the seed bandwidth in dispersion-shifted telecom fiber and to provide a higher-power pump for the final parametric amplification stage installing a supplementary Nd:YVO₄ Innoslab-type amplifier. As a result, 3.7 optical cycle (41.6 fs) pulses at 3.4 μm central wavelength with an energy of 12 μJ at 50 kHz repetition rate were produced^{158,159}. A further increase of

the amplified pulse energy (up to 21.8 μJ) keeping its duration below four optical cycles was achieved by means of an achromatic phase matching (angularly dispersed signal) in the last parametric amplification stage, ensuring extraction of the idler pulse without the angular dispersion¹⁶⁰.

The second OPCPA system¹⁵⁵ was gradually upgraded to a larger output energy introducing additional parametric amplification stage¹⁶¹, higher pulse repetition rate (160 kHz), improved CEP stability¹⁶², and higher peak power¹⁶³, finally producing CEP-stable pulses with a duration of 55 fs (5.4 optical cycles) and energy of 20 μJ at a center wavelength of 3.05 μm ¹⁶⁴. Implementation of all-solid-state self-compression scheme based on filamentation in a YAG crystal yielded pulses as short as 32 fs (2.9 optical cycles). This OPCPA system was shown to provide intrinsically synchronized SWIR output pulses compressible to sub-100 fs, which were readily employed to produce multicolor outputs by means of cascaded frequency up-conversion chain that included non-collinear optical parametric amplification, second harmonic and sum frequency generation stages, involving pump (at 1064 nm), signal (at 3100 nm) and idler (at 1620 nm) pulses¹⁶⁵. Finally, a considerable improvement of the OPCPA output parameters was achieved by adding yet another two parametric amplification stages using KNbO_3 crystals and performing chirp inversion of the seed, which allowed using bulk stretcher as well as bulk compressor, resulting in 21 W average power, 131 μJ pulse energy and 97 fs (sub-9-cycle) pulse duration at a center wavelength of 3.25 μm ¹⁶⁶. Post-compression of these pulses close to a single optical cycle was performed through soliton self-compression inside an argon-filled antiresonant-guiding photonic crystal fiber, yielding pulse width as short as 14.5 fs (1.35 optical cycle) with a peak power of 3.9 GW and an average power of 9.6 W.

A notable effort was dedicated to develop high repetition rate MIR OPCPA systems based on a single driving laser source taking the advantage of robust passive optical synchronization between pump and seed pulses, thus reducing the overall complexity of the system. 100 kHz OPCPA system delivering CEP-stable 4 optical cycle (38-fs) pulses at 3.1 μm with an average power of 4 W was built around an industrial Yb:YAG thin-disk regenerative amplifier¹⁶⁷. Its 1.1 ps pulses were used for both: pumping two-stage optical parametric amplifier, which consisted of MgO:PPLN crystals with fan-out poling and production of CEP-stable MIR seed pulse via

supercontinuum generation in bulk YAG and subsequent DFG between the long wavelength portion of supercontinuum and pump pulses. A further upgrade of this OPCPA system by adding an extra amplification stage based on unpoled LN, resulted in an increase of the output energy by a factor of >4 , yielding an average power of 15.2 W and demonstrating superior long-term performance in terms of shot-to-shot energy, beam pointing and CEP stability over more than 8 hours of continuous operation¹⁶⁸. The output pulses of analogous OPCPA system were post-compressed from 4.7 to 2.3 cycles (23.5 fs) in a hybrid thin plate setup that used a combination of dielectric (YAG) and semiconductor (Si) crystals¹⁶⁹ and, more recently, to sub-two optical cycles (19.6 fs) with addition of dispersive mirrors for fine dispersion compensation¹⁷⁰. 61 fs pulses at 3 μm with an energy of $>300 \mu\text{J}$ were generated from MIR OPCPA system built on the basis of commercial Yb:YAG Innoslab amplifier operating at 10 kHz, that served to simultaneously produce SWIR supercontinuum seed and pump for 4 parametric amplification stages that employed MgO:PPLN and PPSLT crystals¹⁷¹. Further self-compression of the output pulses to 21 fs with 83% energy throughput was achieved by nonlinear propagation in a YAG plate. More recently, this OPCPA system was upgraded by employing more powerful Yb:YAG Innoslab CPA driving laser, replacing PPSLT crystals with KTA in final amplification stages and using engineered flat-top

pump beam in the last amplification stage, resulting in doubled pump-to-idler conversion efficiency¹⁷². The system produced 125 fs pulses (50 fs after post-compression) with an energy of 2.7 mJ and an average power of 27 W, which is the highest average power of the MIR OPCPA systems reported so far, see Fig. 7.

A more sophisticated MIR OPCPA system producing sub-mJ 65 fs, 3 μm pulses at a repetition rate of 100 Hz was built around Ti:sapphire oscillator that seeded both, the pump channel with Yb:YAG Innoslab power amplifier and four-stage OPCPA consisting of two second harmonic-pumped BBO crystals followed by fundamental harmonic-pumped KTA and LiIO₃ crystals, which altogether maintained a broad bandwidth supporting pulses as short as 35 fs, with potential for scaling the repetition rate and average power¹⁷³.

The very first 100 GW-level MIR OPCPA system was built around femtosecond Yb:KGW oscillator with OPA front-end pumped by femtosecond Yb:CaF₂ CPA amplifier, producing seed pulse at the signal (1.46 μm) wavelength and optically synchronized high energy Nd:YAG amplifier, which provided pump for two KTA-based optical parametric amplification stages, demonstrating 83 fs, 8 mJ pulses at the idler wavelength of 3.9 μm ¹⁷⁴. This OPCPA system was further upgraded by using more powerful pump laser and adding third amplification stage (Fig. 8) to produce slightly longer (94 fs), but much more energetic (21 mJ) pulses¹⁷⁵, which were

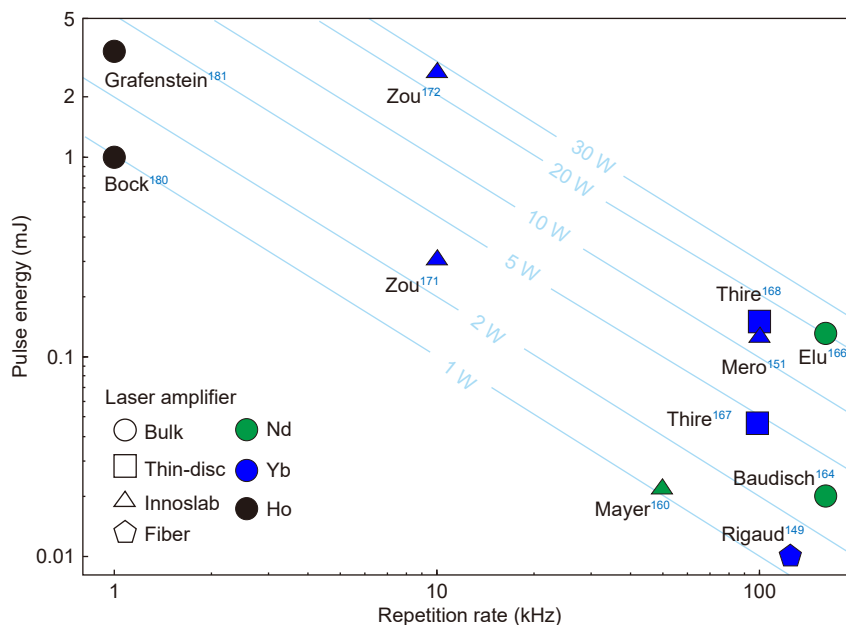


Fig. 7 | Graphical summary of the performance of high average power MIR OPCPA systems. Color coding of data points denotes the gain medium of pump laser, while different shapes indicate the configuration of laser amplifier.

additionally self-compressed down to 30 fs (sub-three optical cycles) by the nonlinear propagation in a 2-mm thick YAG plate, yielding sub-TW (0.44 TW) peak power at the output¹⁷⁶. Wavelength tunable (3.3–3.95 μm) multi-millijoule MIR pulses were produced in OPCPA scheme that used amplified Ti:sapphire laser-pumped OPA as a front-end and electronically synchronized joule-class Nd:YAG boost amplifier serving as a pump source. Single-pass non-collinear optical parametric amplification in LN crystal produced 120 GW pulses with duration of 111 fs and energy of 13.3 mJ at a central wavelength of 3.425 μm ¹⁷⁷. CEP-stable 105 fs, 5.5 mJ pulses at a central wavelength of 4 μm and 100 Hz repetition rate were produced by KTA-based OPCPA, which employed electrically synchronized Ti:sapphire and Nd:YAG lasers¹⁷⁸. Post-compression in krypton gas-filled hollow core fiber yielded a pulse duration of 21.5 fs (1.6 optical cycle) with an energy of 2.6 mJ. Finally, CEP-stable 21 mJ, 70 fs (6.3 optical cycle) pulses at 3.3 μm were produced by dual-chirped optical parametric amplification in MgO:LN with a joule-class Ti:sapphire laser system¹³³, yielding a peak power of 300 GW, which is the highest value of the peak power directly produced by MIR OPCPA system so far, see Fig. 4.

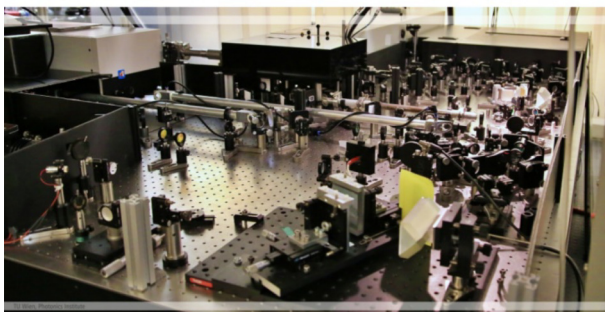
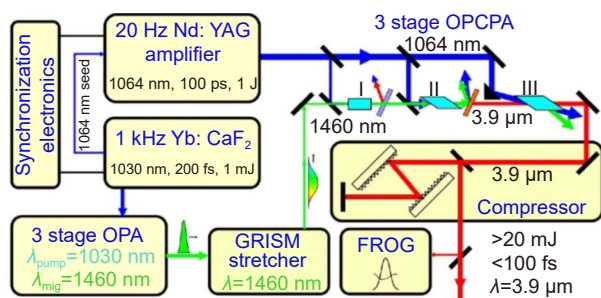


Fig. 8 | Layout of the 3.9 μm OPCPA system. Photo at the bottom: image of the back-end of the system. Image courtesy dr. A. Pugžlys, Photonics Institute, Technical University Wien. Figure reproduced with permission from ref.¹⁷⁵, under a Creative Commons Attribution 4.0 International License.

OPCPA beyond 4 μm

The major difficulties of further OPCPA wavelength scaling arise from increasingly unfavorable pump-to-idler photon ratio, which follows from short ($\sim 1 \mu\text{m}$) pump wavelength provided by Nd and Yb pump lasers and limited transparency of oxide nonlinear crystals in the MIR spectral range. Therefore MIR OPCPA systems operating at wavelengths beyond 4 μm are designed using novel pump sources based on Ho-doped gain media operating around 2 μm and employing non-oxide nonlinear crystals as amplifying media. Out of these, ZGP crystal emerged as particularly attractive nonlinear material for broadband high-energy amplification in the MIR with 2 μm pumping.

To this end, sub-millijoule, multi-GW, few optical cycle (75 fs) pulses at 5.1 μm were produced by OPCPA system which used femtosecond Er: fiber laser providing three-color output as a front-end¹⁷⁹. The broadband seed at 3.4 μm was produced via DFG between the original and spectrally broadened Er: fiber laser outputs, whereas the third spectrally broadened laser output was used to seed 1 kHz picosecond Ho:YLF amplifier, which pumped three-stage ZGP crystal-based optical parametric amplifier. This OPCPA system was further improved to 1 mJ output energy and implemented active phase control by SLM on the signal pulse¹⁸⁰ and eventually, upgraded to four amplification stage configuration, resulting in 89.4 fs, 3.4 mJ pulses at a center wavelength of 4.9 μm with a peak power of 33 GW¹⁸¹, which is the highest figure for OPCPA systems operating beyond 4 μm . More recently, the seeding concept of the above OPCPA scheme was completely changed by incorporating Cr:ZnS master oscillator emitting 40 fs pulses at 2.4 μm as a front-end, which was used to seed both, Ho:YLF regenerative amplifier and two-stage OPCPA based on ZGP crystal¹⁸², see Fig. 9. The resulting idler pulses tunable in the wavelength range of 5.4–6.8 μm were compressed in a simple CaF₂ prism compressor to sub-150 fs duration with $> 400 \mu\text{J}$ energy and a peak power of 3 GW. More recently, dispersion management using bulk material stretching and compression in combination with precise phase shaping prior to amplification enabled compression of idler pulses to a sub-100 fs duration¹⁸³.

Few optical cycle pulses at 7 μm were produced using a conceptually similar OPCPA architecture with Er:Tm:Ho: fiber laser front-end. Ho:YLF amplifier-pumped ZGP OPCPA was seeded by a broadband CEP-stable pulse centered at 7 μm , which was produced via

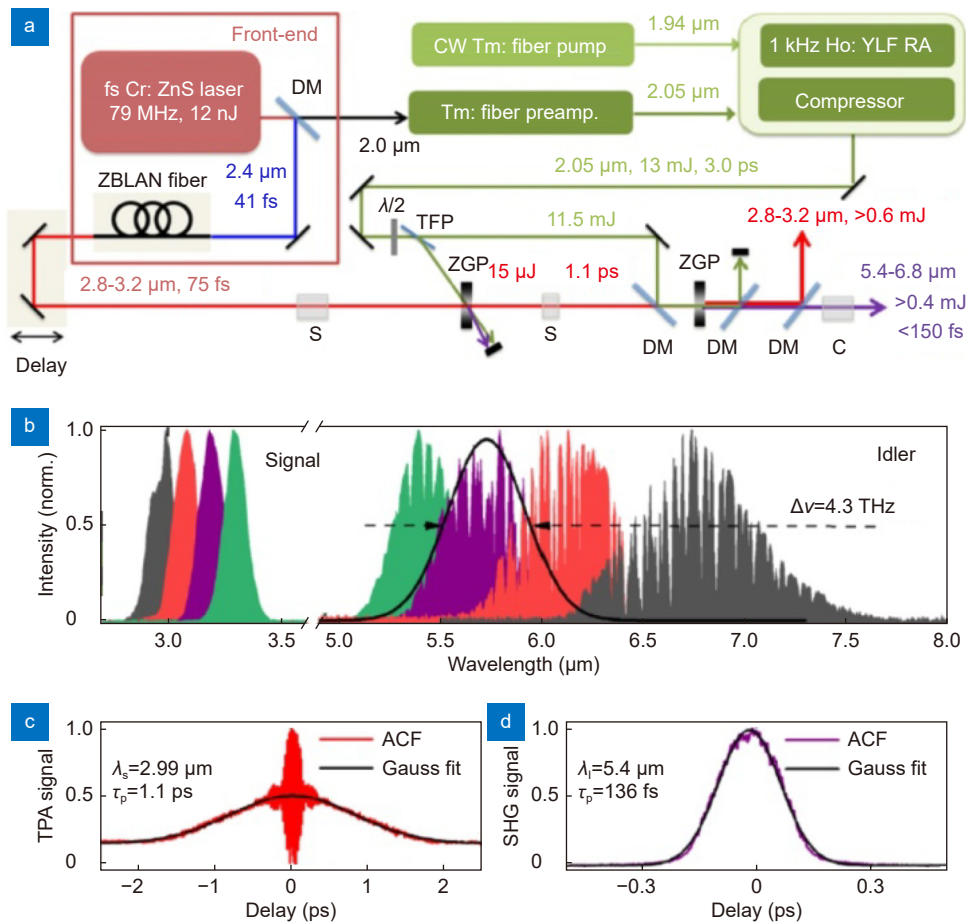


Fig. 9 | (a) Setup of the MIR OPCPA that comprises the front-end including femtosecond Cr:ZnS master oscillator and fluoride fiber (ZBLAN), Ho:YLF regenerative amplifier as pump and two optical parametric amplification stages based on ZGP crystals. (b) Spectral intensities of the signal (left) and the corresponding idler pulses (right). Autocorrelation functions (ACF) of (c) uncompressed signal at 2.99 μm and (d) re-compressed idler pulses at 5.4 μm. Figure reproduced with permission from ref.¹⁸², The Optical Society.

DFG between two spectrally-shifted femtosecond outputs from the Er:Tm:Ho: fiber front-end. The amplified pulses were compressed in a diffraction grating-pair compressor, yielding 180 fs, 200 μJ pulses at the output¹⁸⁴. A further improvement of this OPCPA system was performed by upgrading the pump laser and introducing a chirp inversion stage between the parametric amplification sections, allowing compression of the amplified pulse in a bulk dielectric medium (BaF₂ rod), producing 188 fs (8 optical cycles), 0.75 mJ pulses with a peak power of 3.7 GW¹⁸⁵. Various OPCPA strategies employing ZGP, GaSe and AGSe crystals under pumping around 2 μm were examined numerically, demonstrating prospects of high-peak power few optical cycle pulse generation in the LWIR (8–16 μm) spectral range¹⁸⁶. The numerical studies revealed feasibility of ZGP OPCPA to provide sub-cycle pulses with terawatt peak power in the wavelength range of 4–12 μm under properly tailored phase matching conditions and using either broadband 2.4 μm Cr:ZnSe/ZnS or narrowband 2 μm Ho:YLF pump

lasers¹⁸⁷. So far, few optical cycle pulses with the longest central wavelength of 9 μm were experimentally produced in LiGaS₂ (LGS) crystal-based OPCPA, which was pumped by Yb:YAG laser operating at 10 kHz repetition rate and seeded by NIR supercontinuum generated in a YAG crystal using a small energy fraction from the same laser. Such LWIR OPCPA produced 142 fs (less than five optical cycles) pulses with energy of 14 μJ¹⁸⁸.

Finally, conversion of OPCPA output via intrapulse DFG suggests an alternative method for wavelength scaling further into LWIR region. To this end, generation of sub-three optical cycle pulses with a center wavelength of 8.5 μm was demonstrated with 2.1 μm OPCPA in AGSe crystal¹⁸⁹. More recently, 60 fs (1.8-cycle) pulses centered at 10.3 μm were produced with 3 μm OPCPA in GaSe crystal¹⁹⁰.

Other developments

Diverse experimental OPCPA implementations attested

versatility of the OPCPA concept by demonstrating amplification of ultraviolet femtosecond pulses at 405 nm¹⁹¹ and at 310 nm¹⁹², in the latter case performing four-wave amplification in isotropic solid-state medium (fused silica), as well as producing visible output from OPCPA system with integrated sum-frequency generation stage¹⁹³. An interesting idea was proposed of using compressed SWIR (at 1.6 μm) and uncompressed MIR (at 3.1 μm) outputs from KTA-based OPCPA system as pump and seed, respectively, for subsequent OPCPA system based on LiGaSe₂ crystal operating at the degeneracy¹⁹⁴.

A possibility of OPCPA to amplify complex-shaped wave packets was studied numerically, demonstrating that broadband X-pulses with specific spatial and temporal chirps can be efficiently amplified without phase distortions and self-compressed during free-space propagation onto the target area¹⁹⁵. Very recently, amplification of chirped vortex pulse at 4 μm to multi-mJ energy and its compression to less than 9 optical cycles was experimentally demonstrated in OPCPA system based on KTA crystal¹⁹⁶.

A particularly interesting development line addresses application of the OPCPA technique to all-fiber systems. Unlike conventional OPCPA, where optical parametric amplification is performed in bulk crystals with second-order nonlinearity, fiber OPCPA (FOPCPA) uses highly nonlinear optical fiber with cubic nonlinearity as an amplifying medium¹⁹⁷, hence offering stability and versatility of fiber setups, and multi-MHz repetition rates that are accessible with the state-of-the-art fiber lasers. Since the first experimental demonstration of femtosecond FOPCPA in photonic crystal fiber (PCF) around 1 μm ¹⁹⁸, the subsequent FOPCPA realizations extended wavelength range into telecom window (around 1.55 μm) in picosecond¹⁹⁹, sub-picosecond²⁰⁰ and femtosecond²⁰¹ operation regimes, using highly nonlinear fibers (HNLF) as amplifying media. Numerical studies suggested that the achievable FOPCPA bandwidth can be twice as large as in standard setups making use of two-pump configuration, which is capable of delivering pulses as short as 15 fs, paving the way toward all-fiber amplification of few optical cycle pulses²⁰². The follow-up studies considered FOPCPA pumping by chirped pulses, which induce temporally spread spectral gain, and may produce very high (45–60 dB) gain within a very broad spectral bandwidth around 1 μm , supporting amplification of sub-30 fs pulses^{203–205}. FOPCPA in a normally dis-

persive PCF enabled amplification of femtosecond pulses at wavelengths which are relatively far (signal at 0.85 μm and idler at 1.3 μm) from the pump wavelength (1.03 μm)²⁰⁶, also demonstrating that the signal and idler waves can be widely customized by proper arrangement of the relationships between the chirps of the pump and seed pulses and parametric gain²⁰⁷. FOPCPA with very high gain (more than 55 dB), overall pump-to-signal conversion close to 50% and μJ signal energy was demonstrated in a solid core photonic bandgap (PBG) fiber with a large mode area²⁰⁸, while 70 fs pulses were produced in FOPCPA via birefringence phase matching in a step-index single-mode optical fiber²⁰⁹. Finally, watt-level FOPCPA systems providing femtosecond pulses at 1.3 μm ²¹⁰ and 1.7 μm ²¹¹, were elaborated recently, aiming at applications in bio-photonics and biomedical treatment.

Applications

Table-top OPCPA systems currently provide the shortest pulses in the optical range, offering a wide choice of driving wavelengths, which are ideally suited to experimentally investigate highly nonlinear processes in atomic, molecular, plasma, and solid-state physics. OPCPA systems serve as driving sources for strong field phenomena in noble gas jets, such as laser plasma acceleration²¹² and high harmonic generation (HHG)^{124,213,214}, with an emphasis for excitation of coherent electromagnetic waves far beyond the optical spectrum, producing attosecond bursts in the extreme ultraviolet and soft X-ray range, and so emerging as compact alternatives to synchrotron radiation and free-electron lasers. To this end, soft X-ray production in a water window^{104,107,119,125,128,135,215–218}, and generation of single isolated attosecond pulses^{219–221} and attosecond pulse trains²²² have been reported with diverse OPCPA systems. MIR OPCPA-driven generation of high brightness supercontinuum of ultrahigh harmonics up to unprecedented orders greater than 5000, potentially allowing the generation of pulses as short as 2.5 attoseconds was reported²²³, see Fig. 10, which also provides an illustrative comparison of HHG supercontinua produced with few optical cycle pulses with central wavelengths of 0.8, 1.3, 2.0 and 3.9 μm . Table-top HHG sources driven by OPCPA systems were employed for water-window X-ray imaging²²⁴ and soft X-ray spectroscopy²²⁵. More recently, the generated ultrabroadband high harmonic supercontinua were applied for X-ray absorption spectroscopy at

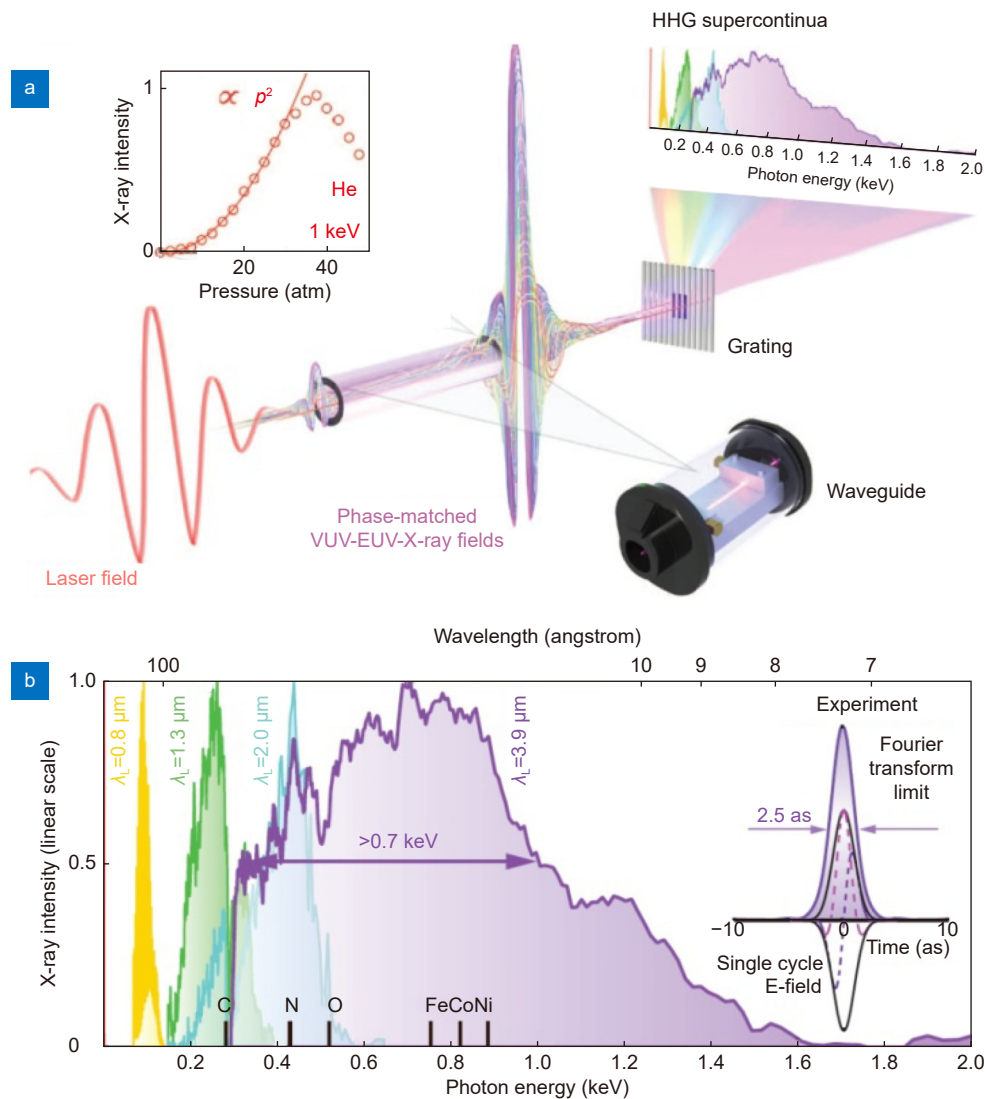


Fig. 10 | (a) Schematic illustration of the coherent kilo-electronvolt X-ray supercontinua emitted when a MIR laser pulse is focused into a high-pressure He gas-filled waveguide, where phase-matched harmonic signal grows quadratically with pressure. (b) Experimental HHG spectra emitted under full phase-matching conditions as a function of driving wavelength (yellow: 0.8 μm ; green: 1.3 μm ; blue: 2.0 μm ; purple: 3.9 μm). Inset: Fourier transform-limited pulse duration of 2.5 as. Figure reproduced with permission from ref.²²³, AAAS.

the K- and L-absorption edges of solids and in the water window, allowing for probing the fastest processes on femtosecond-to-attosecond time scales and picometer length scales²²⁶. OPCPA sources have also been demonstrated as indispensable tools for performing CEP-sensitive experiments for the study and control of ultrafast processes in light-matter interactions²²⁷. Moreover, OPCPA sources were demonstrated to efficiently drive HHG generation from solid surfaces^{78,171,228}, hard X-ray production from metallic targets²²⁹ and for photoemission spectroscopy of solids²³⁰. OPCPA combined with reaction microscope enabled to visualize strong-field interactions and electron recollisions in three dimensions that are the core process driving strong-field phenomena, al-

lowing to probe atomic structure via laser-induced electron diffraction^{231,232}. More recently, OPCPA sources were used for laser plasma wakefield acceleration, reporting electron acceleration up to MeV-scale and relativistic self-focusing in gas jets²³³, and observation of relativistic effects in plasma from solid targets²³⁴.

Since few optical cycle OPCPA systems deliver ultrabroadband spectra exceeding an optical octave and allow accurate control of spectral phase, precisely synchronized OPCPA systems readily serve for coherent sub-cycle optical waveform synthesis offering several distinct advantages over other existing methods²³⁵. In that regard, full phase and amplitude control enables the generation of sub-optical-cycle pulses with a desired electric

field profile, or more generally, any optical waveform supported by the amplified spectrum with scalability of average^{236,237} and peak²³⁸ powers. These features are of great importance for optimizing the HHG process and achieving high energy isolated attosecond pulses²³⁹, so opening a route to a completely new regime of light-matter interaction, the so called waveform nonlinear optics.

High repetition rate MIR OPCPA systems serve as versatile tools for many experiments in multidimensional spectroscopy in the molecular fingerprint region²⁴⁰. For example, a 100 kHz OPCPA system, which employed difference frequency generation and subsequent pulse shaping, was used to deliver pulse pairs, resulting in millisecond 2D spectral acquisition times which enable experiments in 2D IR microscopy and nanoscopy²⁴¹. Such systems also offer an excellent performance in running ultra-stable shot-to-shot statistical measurements over a long term¹⁶⁸, whereas OPCPA systems, which produce simultaneous optically synchronized outputs at various wavelengths, enable time-resolved investigation of electron and nuclear dynamics during photochemical reactions and high-energy above-threshold ionization phenomena¹⁶⁵. Adiabatic difference frequency generation in aperiodically poled grating in a magnesium-oxide-doped congruent LN crystal employing OPCPA output pulses²⁴² resulted in production of almost single-cycle pulses in the optical range²⁴³. Proper pulse shaping applied to such scheme allows the generation of closely (within a few picoseconds) delayed pairs of fully compressible MIR pulses, which could be further used for two-dimensional spectroscopy exceeding an octave-spanning bandwidth.

Availability of high peak power OPCPA systems enabled to perform cutting-edge experiments in the emerging field of ultrafast mid-infrared nonlinear optics. Observations of nonlinear optical phenomena induced by propagation of high power ultrashort MIR pulses in gaseous media proposed a new look at filamentation physics and nonlinear optics in gaseous media¹⁷⁵, demonstrating production of high-energy ultrabroadband supercontinua in noble gases²⁴⁴, atmospheric air²⁴⁵ and its individual constituents²⁴⁶. A remarkable spectral extension towards the short-wavelength side due to generation of multiple odd harmonics was observed, which was considered as a tool for probing higher order Kerr effect, related optical nonlinearities and key optical constants of the media²⁴⁷. Remote initiation of backward lasing from molecular gases by MIR filaments²⁴⁸ and its use

for gas sensing²⁴⁹ were demonstrated as well. Various pulse compression regimes delivering high power compressed pulses on remote targets were unveiled^{250–253} thanks to precise mapping of anomalous dispersion of air in the 3.6–4.2 μm range²⁵⁴. Novel aspects of nonlinear propagation and pulse self-compression in bulk materials and fibers were uncovered^{255–258}, demonstrating multioctave, CEP-stable supercontinua with a potential self-compression of spectrally broadened pulses down to a single optical cycle.

OPCPA-driven light sources with unprecedented spectral bandwidths were demonstrated recently, offering new opportunities for diverse applications in biochemical sensing, time-resolved spectroscopy and attosecond light-wave electronics²⁵⁹. Coherent and ultrabroadband comb covering seven optical octaves from 340 nm to 40 μm , with CEP-stable electric field waveforms corresponding to sub-three-optical-cycle pulses was demonstrated with MIR OPCPA at 3.2 μm and combining soliton self-compression and dispersive wave generation in an anti-resonant-reflection photonic-crystal fiber with intra-pulse DFG²⁶⁰. Focusing two-color field, consisting of the 3.9 μm OPCPA output and its second harmonic into a gas target, produced bright multiband SC radiation, spanning over 14 octaves, from below 300 nm in the UV all the way beyond 4.3 mm, in the millimeter-wave frequency band²⁶¹, as shown in Fig. 11. In particular, it was demonstrated that THz to millimeter-wave part of the spectrum is emitted in the form of half-cycle field waveforms that can be focused to yield field strengths of 5 MV/cm. Intense sub-cycle THz pulses with sub-millijoule energy and THz conversion efficiency of 2.36%, resulting in THz field amplitudes above 100 MV/cm were produced by co-filamentation of 3.9 μm OPCPA output and its second harmonic in ambient air, paving the way toward free space extreme nonlinear THz optics using table-top laser systems²⁶². More recently, record optical-to-THz conversion efficiencies approaching 6% were produced by optical rectification in organic DAST (4-N,N-dimethylamino-4'-N'-methyl-stilbazolum tosylate) crystal using the same OPCPA source²⁶³.

Last, but not the least, high peak power OPCPA pulses were employed for performing damage tests of various optical components and coatings, which are vital in designing petawatt laser systems²⁶⁴. Frequency doubled NIR OPCPA output was considered to provide high quality, high contrast seed pulses for the multi-terawatt ultrashort pulse excimer amplifier operating in the blue

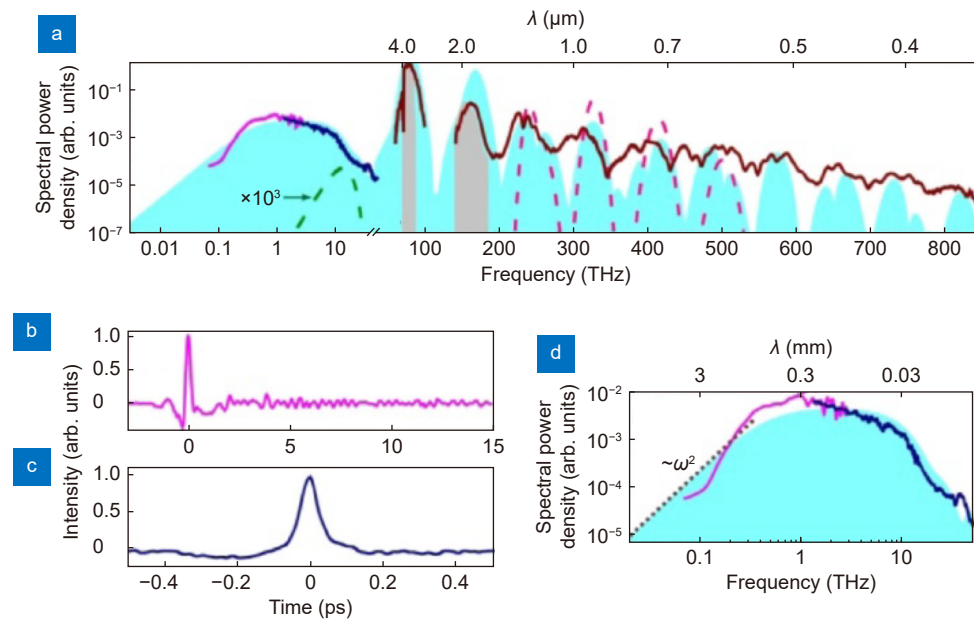


Fig. 11 | (a) Spectrum of the millimeter-wave-to-ultraviolet supercontinuum. (b) Electro-optic sampling and (c) autocorrelation traces of the waveforms of the THz-millimeter-wave field. (d) The millimeter-wave-to-THz part of the supercontinuum spectrum. Figure reproduced with permission from ref.²⁶¹, The Optical Society.

(475 nm)²⁶⁵, whereas the third and fourth harmonics of a tunable, burst mode OPCPA with center wavelengths ranging from 720 to 900 nm and pulse energies up to 1.12 mJ were considered for seeding high repetition rate free-electron lasers¹¹².

Conclusions

Tremendous progress of table-top OPCPA systems during the past decade was spurred by recent scientific and technological advances in laser science and ultrafast nonlinear optics. In particular, the developments of solid-state laser oscillator and amplifier technology opened new perspectives for OPCPA seeding and pumping in diverse regimes of energy, pulsewidth, wavelength and repetition rate. The availability of advanced pump sources made feasible the design of compact TW-class OPCPA systems offering the combination of high peak and high average powers, which represents an important frontier in contemporary laser science itself, and, on the other hand, promoted the development of high average power OPCPA systems operating at multi-kHz to 100s kHz repetition rates, allowing to perform diverse experiments in, e.g. strong field physics, in compact setups with sufficient detection sensitivity and high signal-to-noise ratio. The advances of broadband seed generation techniques, availability of existing and growth of novel nonlinear optical crystals with suitable optical properties and inception novel pump sources based on Ho-doped lasing ma-

terials made possible unprecedented coverage of carrier wavelengths offered by OPCPA systems. Eventually, modern pulse post-compression techniques appeared especially efficient in the MIR spectral range, allowing further shortening of the generated pulses by relatively simple means. Successful experimental realization of MIR OPCPA systems established a solid background for ongoing efforts in shifting the OPCPA output wavelengths further into the long-wave infrared; a very challenging task guided by motivation to perform cutting-edge research in strong field physics and attosecond science that benefit from large ponderomotive energy, which scales as squared wavelength of the driving source.

To summarize the present-day state of the art, table-top OPCPA systems represent a unique class of few optical cycle light sources that reached high level of maturity, establishing a solid experimental platform for research in diverse fields of ultrafast science, as already attested by a wealth of fascinating applications with much more to come in the nearest future.

References

1. Strickland D, Mourou G. Compression of amplified chirped optical pulses. *Opt Commun* **56**, 219–221 (1985).
2. Mourou G. Nobel Lecture: extreme light physics and application. *Rev Mod Phys* **91**, 030501 (2019).
3. Dubietis A, Jonušauskas G, Piskarskas A. Powerful femtosecond pulse generation by chirped and stretched pulse parametric amplification in BBO crystal. *Opt Commun* **88**, 437–440

- (1992).
4. Cerullo G, De Silvestri S. Ultrafast optical parametric amplifiers. *Rev Sci Instrum* **74**, 1–18 (2003).
 5. Brida D, Manzoni C, Cirmi G, Marangoni M, Bonora S et al. Few-optical-cycle pulses tunable from the visible to the mid-infrared by optical parametric amplifiers. *J Opt* **12**, 013001 (2010).
 6. Manzoni C, Cerullo G. Design criteria for ultrafast optical parametric amplifiers. *J Opt* **18**, 103501 (2016).
 7. Butkus R, Danielius R, Dubietis A, Piskarskas A, Stabinis A. Progress in chirped pulse optical parametric amplifiers. *Appl Phys B* **79**, 693–700 (2004).
 8. Dubietis A, Butkus R, Piskarskas AP. Trends in chirped pulse optical parametric amplification. *IEEE J Sel Top Quantum Electron* **12**, 163–172 (2006).
 9. Witte S, Eikema KSE. Ultrafast optical parametric chirped-pulse amplification. *IEEE J Sel Top Quantum Electron* **18**, 296–307 (2012).
 10. Vaupel A, Bodnar N, Webb B, Shah L, Richardson MC. Concepts, performance review, and prospects of table-top, few-cycle optical parametric chirped-pulse amplification. *Opt Eng* **53**, 051507 (2013).
 11. Rothhardt J, Hädrich S, Delagnes JC, Cormier E, Limpert J. High average power near-infrared few-cycle lasers. *Laser Photon Rev* **11**, 1700043 (2017).
 12. Ciriolo AG, Negro M, Devetta M, Cinquanta E, Faccialà D et al. Optical parametric amplification techniques for the generation of high-energy few-optical-cycles IR pulses for strong field applications. *Appl Sci* **7**, 265 (2017).
 13. Danson CN, Haefner C, Bromage J, Butcher T, Chanteloup JCF et al. Petawatt and exawatt class lasers worldwide. *High Power Laser Sci Eng* **7**, e54 (2019).
 14. Pires H, Baudisch M, Sanchez D, Hemmer M, Biegert J. Ultrashort pulse generation in the mid-IR. *Prog Quantum Electron* **43**, 1–30 (2015).
 15. Fattahi H, Barros HG, Gorjan M, Nubbemeyer T, Alsaif B et al. Third-generation femtosecond technology. *Optica* **1**, 45–63 (2014).
 16. Piskarskas A, Stabinis A, Yankauskas A. Phase phenomena in parametric amplifiers and generators of ultrashort light pulses. *Sov Phys Usp* **29**, 869–879 (1986).
 17. Ross IN, Matousek P, Towrie M, Langley AJ, Collier JL. The prospects for ultrashort pulse duration and ultrahigh intensity using optical parametric chirped pulse amplifiers. *Opt Commun* **144**, 125–133 (1997).
 18. Ross IN, Matousek P, Towrie M, Langley AJ, Collier JL et al. Prospects for a multi-PW source using optical parametric chirped pulse amplifiers. *Laser Part Beams* **17**, 331–340 (1999).
 19. Ross IN, Collier JL, Matousek P, Danson CN, Neely D et al. Generation of terawatt pulses by use of optical parametric chirped pulse amplification. *Appl Opt* **39**, 2422–2427 (2000).
 20. Yang XD, Xu ZZ, Leng YX, Lu HH, Lin LH et al. Multiterawatt laser system based on optical parametric chirped pulse amplification. *Opt Lett* **27**, 1135–1137 (2002).
 21. Chekhlov OV, Collier JL, Ross IN, Bates PK, Notley M et al. 35J broadband femtosecond optical parametric chirped pulse amplification system. *Opt Lett* **31**, 3665–3667 (2006).
 22. Lozhkarev VV, Freidman GI, Ginzburg VN, Katin EV, Khazanov EA et al. Compact 0.56 Petawatt laser system based on optical parametric chirped pulse amplification in KD*P crystals. *Laser Phys Lett* **4**, 421–427 (2007).
 23. Yu LH, Liang XY, Xu L, Li WQ, Peng C et al. Optimization for high-energy and high-efficiency broadband optical parametric chirped-pulse amplification in LBO near 800 nm. *Opt Lett* **40**, 3412–3415 (2015).
 24. Zeng XM, Zhou KN, Zuo YL, Zhu QH, Su JQ et al. Multi-petawatt laser facility fully based on optical parametric chirped-pulse amplification. *Opt Lett* **42**, 2014–2017 (2017).
 25. Galletti M, Oliveira P, Galimberti M, Ahmad M, Archipovaite G et al. Ultra-broadband all-OPCPA petawatt facility fully based on LBO. *High Power Laser Sci Eng* **8**, e31 (2020).
 26. Jovanovic I, Comaskey BJ, Ebberts CA, Bonner RA, Pennington DM et al. Optical parametric chirped-pulse amplifier as an alternative to Ti: sapphire regenerative amplifiers. *Appl Opt* **41**, 2923–2929 (2002).
 27. Hauri CP, Schlup P, Arisholm G, Biegert J, Keller U. Phase-preserving chirped-pulse optical parametric amplification to 17.3 fs directly from a Ti: sapphire oscillator. *Opt Lett* **29**, 1369–1371 (2004).
 28. Kakehata M, Takada H, Kobayashi Y, Torizuka K, Takamiya H et al. Carrier-envelope-phase stabilized chirped-pulse amplification system scalable to higher pulse energies. *Opt Express* **12**, 2070–2080 (2004).
 29. Xu L, Tempea G, Poppe A, Lenzner M, Spielmann C et al. High-power sub-10-fs Ti: sapphire oscillators. *Appl Phys B* **65**, 151–159 (1997).
 30. Ell R, Morgner U, Kärtner FX, Fujimoto JG, Ippen EP et al. Generation of 5-fs pulses and octave-spanning spectra directly from a Ti: sapphire laser. *Opt Lett* **26**, 373–375 (2001).
 31. Dudley J M, Genty G, Coen S. Supercontinuum generation in photonic crystal fiber. *Rev Mod Phys* **78**, 1135–1184 (2006).
 32. Dubietis A, Tamošauskas G, Šuminas R, Jukna V, Couairon A. Ultrafast supercontinuum generation in bulk condensed media. *Lith J Phys* **57**, 113–157 (2017).
 33. Nisoli M, Stagira S, De Silvestri S, Svelto O, Sartania S et al. A novel-high energy pulse compression system: generation of multigigawatt sub-5-fs pulses. *Appl Phys B* **65**, 189–196 (1997).
 34. Fuji T, Apolonski A, Krausz F. Self-stabilization of carrier-envelope offset phase by use of difference-frequency generation. *Opt Lett* **29**, 632–634 (2004).
 35. Adamonis J, Antipenkov R, Kolenda J, Michailovas A, Piskarskas AP et al. High-energy Nd: YAG-amplification system for OPCA pumping. *Quantum Electron* **42**, 567–574 (2012).
 36. Su HP, Peng YJ, Chen JC, Li YY, Wang PF et al. A high-energy, 100 Hz, picosecond laser for OPCA pumping. *Appl Sci* **7**, 997 (2017).
 37. Yang SS, Cui ZJ, Sun ZM, Zhang P, Liu DA. Compact 50 W all-solid-state picosecond laser system at 1 kHz. *Appl Sci* **10**, 6891 (2020).
 38. Mecseki K, Bigourd D, Patankar S, Stuart NH, Smith RA. Flat-top picosecond pulses generated by chirped spectral modulation from a Nd: YLF regenerative amplifier for pumping few-cycle optical parametric amplifiers. *Appl Opt* **53**, 2229–2235 (2014).
 39. Heese C, Oehler AE, Gallmann L, Keller U. High-energy picosecond Nd: YVO₄ slab amplifier for OPCA pumping. *Appl Phys B* **103**, 5–8 (2011).
 40. Hemmer M, Vaupel A, Wohlmuth M, Richardson M. OPCA

- pump laser based on a regenerative amplifier with volume Bragg grating spectral filtering. *Appl Phys B* **106**, 599–603 (2012).
41. Liu JX, Wang W, Wang ZH, Lv ZG, Zhang ZY et al. Diode-pumped high energy and high average power all-solid-state picosecond amplifier systems. *Appl Sci* **5**, 1590–1602 (2015).
 42. Michailovas K, Zaukevičius A, Petrauskienė V, Smilgevičius V, Balickas S et al. Sub-20 ps high energy pulses from 1 kHz Neodymium-based CPA. *Lith J Phys* **58**, 159–169 (2018).
 43. Vaupel A, Bodnar N, Webb B, Shah L, Hemmer M et al. Hybrid master oscillator power amplifier system providing 10 mJ, 32 W, and 50 MW pulses for optical parametric chirped-pulse amplification pumping. *J Opt Soc Am B* **30**, 3278–3283 (2013).
 44. Michailovas K, Baltuska A, Pugzlys A, Smilgevičius V, Michailovas A et al. Combined Yb/Nd driver for optical parametric chirped pulse amplifiers. *Opt Express* **24**, 22261–22271 (2016).
 45. Antipenkov R, Varanavičius A, Zaukevičius A, Piskarskas AP. Femtosecond Yb: KGW MOPA driven broadband NOPA as a frontend for TW few-cycle pulse systems. *Opt Express* **19**, 3519–3524 (2011).
 46. João CP, Wagner F, Körner J, Hein J, Gottschall T et al. A 10-mJ-level compact CPA system based on Yb: KGW for ultrafast optical parametric amplifier pumping. *Appl Phys B* **118**, 401–407 (2015).
 47. Klingebiel S, Wandt C, Skrobel C, Ahmad I, Trushin SA et al. High energy picosecond Yb: YAG CPA system at 10 Hz repetition rate for pumping optical parametric amplifiers. *Opt Express* **19**, 5357–5363 (2011).
 48. Eidam T, Rothhardt J, Stutzki F, Jansen F, Hädrich S et al. Fiber chirped-pulse amplification system emitting 3.8 GW peak power. *Opt Express* **19**, 255–260 (2011).
 49. Zapata LE, Reichert F, Hemmer M, Kärtner FX. 250 W average power, 100 kHz repetition rate cryogenic Yb: YAG amplifier for OPCPA pumping. *Opt Lett* **41**, 492–495 (2016).
 50. Mackonis P, Rodin AM. Laser with 1.2 ps, 20 mJ pulses at 100 Hz based on CPA with a low doping level Yb: YAG rods for seeding and pumping of OPCPA. *Opt Express* **28**, 1261–1268 (2020).
 51. Hubka Z, Antipenkov R, Boge R, Erdman E, Greco M et al. 120 mJ, 1 kHz, picosecond laser at 515 nm. *Opt Lett* **24**, 5655–5658 (2021).
 52. Schulz M, Riedel R, Willner A, Mans T, Schnitzler C et al. Yb: YAG Innoslab amplifier: efficient high repetition rate subpicosecond pumping system for optical parametric chirped pulse amplification. *Opt Lett* **36**, 2456–2458 (2011).
 53. Schmidt BE, Hage A, Mans T, Légaré F, Wörner HJ. Highly stable, 54mJ Yb-InnoSlab laser platform at 0.5kW average power. *Opt Express* **25**, 17549–17555 (2017).
 54. Malevich P, Andriukaitis G, Flöry T, Verhoef AJ, Fernández A et al. High energy and average power femtosecond laser for driving mid-infrared optical parametric amplifiers. *Opt Lett* **38**, 2746–2749 (2013).
 55. Hemmer M, Sánchez D, Jelínek M, Smirnov V, Jelinkova H et al. 2- μ m wavelength, high-energy Ho: YLF chirped-pulse amplifier for mid-infrared OPCPA. *Opt Lett* **40**, 451–454 (2015).
 56. von Grafenstein L, Bock M, Ueberschaer D, Griebner U, Elsaesser T. Picosecond 34 mJ pulses at kHz repetition rates from a Ho: YLF amplifier at 2 μ m wavelength. *Opt Express* **23**, 33142–33149 (2015).
 57. von Grafenstein L, Bock M, Ueberschaer D, Koç A, Griebner U et al. 2.05 μ m chirped pulse amplification system at a 1 kHz repetition rate-2.4 ps pulses with 17 GW peak power. *Opt Lett* **45**, 3836–3839 (2020).
 58. Prandolini MJ, Riedel R, Schulz M, Hage A, Höppner H et al. Design considerations for a high power, ultrabroadband optical parametric chirped-pulse amplifier. *Opt Express* **22**, 1594–1607 (2014).
 59. Riedel R, Rothhardt J, Beil K, Gronloh B, Klenke A et al. Thermal properties of borate crystals for high power optical parametric chirped-pulse amplification. *Opt Express* **22**, 17607–17619 (2014).
 60. Galletti M, Pires H, Hariton V, Alves J, Oliveira P et al. Ultrabroadband near-infrared NOPAs based on the nonlinear crystals BiBO and YCOB. *High Power Laser Sci Eng* **8**, e29 (2020).
 61. Baudisch M, Hemmer M, Pires H, Biegert J. Performance of MgO: PPLN, KTA, and KNbO₃ for mid-wave infrared broadband parametric amplification at high average power. *Opt Lett* **39**, 5802–5805 (2014).
 62. Schunemann PG, Zawilski KT, Pomeranz LA, Creedon DJ, Budni PA. Advances in nonlinear optical crystals for mid-infrared coherent sources. *J Opt Soc Am B* **33**, D36–D43 (2016).
 63. Tian K, He LZ, Yang XM, Liang HK. Mid-infrared few-cycle pulse generation and amplification. *Photonics* **8**, 290 (2021).
 64. Liu JS, Ma JG, Wang J, Yuan P, Xie GQ et al. Toward 5.2 μ m terawatt few-cycle pulses via optical parametric chirped-pulse amplification with oxide La₃Ga₅Nb_{0.5}O₁₄ crystals. *High Power Laser Sci Eng* **7**, e61 (2019).
 65. Namboodiri M, Luo C, Indorf G, Golz T, Grguraš I et al. Optical properties of Li-based nonlinear crystals for high power mid-IR OPCPA pumped at 1 μ m under realistic operational conditions. *Opt Mater Express* **11**, 231–239 (2021).
 66. Zinkstok RT, Witte S, Hogervorst W, Eikema KSE. High-power parametric amplification of 11.8-fs laser pulses with carrier-envelope phase control. *Opt Lett* **30**, 78–80 (2005).
 67. Witte S, Zinkstok RT, Hogervorst W, Eikema KSE. Generation of few-cycle terawatt light pulses using optical parametric chirped pulse amplification. *Opt Express* **13**, 4903–4908 (2005).
 68. Ishii N, Turi L, Yakovlev VS, Fuji T, Krausz F et al. Multimillijoule chirped parametric amplification of few-cycle pulses. *Opt Lett* **30**, 567–569 (2005).
 69. Stepanenko Y, Radzewicz C. Multipass non-collinear optical parametric amplifier for femtosecond pulses. *Opt Express* **14**, 779–785 (2006).
 70. Witte S, Zinkstok RT, Wolf AL, Hogervorst W, Ubachs W et al. A source of 2 terawatt, 2.7 cycle laser pulses based on noncollinear optical parametric chirped pulse amplification. *Opt Express* **14**, 8168–8177 (2006).
 71. Wnuk P, Stepanenko Y, Radzewicz C. Multi-terawatt chirped pulse optical parametric amplifier with a time-shear power amplification stage. *Opt Express* **17**, 15264–15273 (2009).
 72. Tavella F, Marcinkevičius A, Krausz F. 90 mJ parametric chirped pulse amplification of 10 fs pulses. *Opt Express* **14**, 12822–12827 (2006).
 73. Tavella F, Nomura Y, Veisz L, Pervak V, Marcinkevičius A et al. Dispersion management for a sub-10-fs, 10 TW optical parametric chirped-pulse amplifier. *Opt Lett* **32**, 2227–2229 (2007).

74. Kiriya H, Mori M, Nakai Y, Yamamoto Y, Tanoue M et al. High-energy, high-contrast, multiterawatt laser pulses by optical parametric chirped-pulse amplification. *Opt Lett* **32**, 2315–2317 (2007).
75. Herrmann D, Veisz L, Tautz R, Tavella F, Schmid K et al. Generation of sub-three-cycle, 16 TW light pulses by using noncollinear optical parametric chirped-pulse amplification. *Opt Lett* **34**, 2459–2461 (2009).
76. Liu XD, Xu L, Zhang M, Pan SL, Liang XY. Broadband optical parametric chirped pulse amplification in $K_3B_6O_{10}Br$ crystal near 800 nm. *Laser Phys Lett* **14**, 095403 (2017).
77. Yang SH, Liang X, Xie XL, Yang QW, Tu XN et al. Ultra-broadband high conversion efficiency optical parametric chirped-pulse amplification based on YCOB crystals. *Opt Express* **28**, 11645–11651 (2020).
78. Kessel A, Leshchenko VE, Jahn O, Krüger M, Münzer A et al. Relativistic few-cycle pulses with high contrast from picosecond-pumped OPCPA. *Optica* **5**, 434–442 (2018).
79. Adachi S, Ishii H, Kanai T, Ishii N, Kosuge A et al. 1.5 mJ, 6.4 fs parametric chirped-pulse amplification system at 1 kHz. *Opt Lett* **32**, 2487–2489 (2007).
80. Adachi S, Ishii N, Kanai T, Kosuge A, Itatani J et al. 5-fs, multi-mJ, CEP-locked parametric chirped-pulse amplifier pumped by a 450-nm source at 1 kHz. *Opt Express* **16**, 14341–14352 (2008).
81. Adachi S, Ishii N, Nomura Y, Kobayashi Y, Itatani J et al. 1.2 mJ sub-4-fs source at 1 kHz from an ionizing gas. *Opt Lett* **35**, 980–982 (2010).
82. Batysta F, Antipenkov R, Green JT, Naylon JA, Novák J et al. Pulse synchronization system for picosecond pulse-pumped OPCPA with femtosecond-level relative timing jitter. *Opt Express* **22**, 30281–30286 (2014).
83. Batysta F, Antipenkov R, Novák J, Green JT, Naylon JA et al. Broadband OPCPA system with 11 mJ output at 1 kHz, compressible to 12 fs. *Opt Express* **24**, 17843–17848 (2016).
84. Bakule P, Antipenkov R, Novák J, Batysta F, Boge R et al. Readiness of L1 ALLEGRA laser system for user operation at ELI beamlines. In *OSA High-brightness Sources and Light-driven Interactions Congress 2020 HF1B. 7* (OSA, 2020).
85. Prinz S, Schnitzenbaumer M, Potamianos D, Schultze M, Stark S et al. Thin-disk pumped optical parametric chirped pulse amplifier delivering CEP-stable multi-mJ few-cycle pulses at 6 kHz. *Opt Express* **26**, 1108–1124 (2018).
86. Stanislauskas T, Budriūnas R, Antipenkov R, Zaukevičius A, Adamonis J et al. Table top TW-class OPCPA system driven by tandem femtosecond Yb: KGW and picosecond Nd: YAG lasers. *Opt Express* **22**, 1865–1870 (2014).
87. Budriūnas R, Stanislauskas T, Varanavičius A. Passively CEP-stabilized frontend for few cycle terawatt OPCPA system. *J Opt* **17**, 094008 (2015).
88. Budriūnas R, Stanislauskas T, Adamonis J, Aleknavičius A, Veitas G et al. 53 W average power CEP-stabilized OPCPA system delivering 5.5 TW few cycle pulses at 1 kHz repetition rate. *Opt Express* **25**, 5797–5806 (2017).
89. Toth S, Stanislauskas T, Balciunas I, Budriūnas R, Adamonis J et al. SYLOS lasers – the frontier of few-cycle, multi-TW, kHz lasers for ultrafast applications at extreme light infrastructure attosecond light pulse source. *J Phys Photonics* **2**, 045003 (2020).
90. Kretschmar M, Tuemmler J, Schütte B, Hoffmann A, Senfftleben B et al. Thin-disk laser-pumped OPCPA system delivering 4.4 TW few-cycle pulses. *Opt Express* **28**, 34574–34585 (2020).
91. Danilevičius R, Zaukevičius A, Budriūnas R, Michailovas A, Rusteika N. Femtosecond wavelength-tunable OPCPA system based on picosecond fiber laser seed and picosecond DPSS laser pump. *Opt Express* **24**, 17532–17540 (2016).
92. Rothhardt J, Hädrich S, Limpert J, Tünnermann A. 80 kHz repetition rate high power fiber amplifier flat-top pulse pumped OPCPA based on BiB_3O_6 . *Opt Express* **17**, 2508–2517 (2009).
93. Rothhardt J, Hädrich S, Gottschall T, Clausnitzer T, Limpert J et al. Compact fiber amplifier pumped OPCPA system delivering gigawatt peak power 35 fs pulses. *Opt Express* **17**, 24130–24136 (2009).
94. Tavella F, Willner A, Rothhardt J, Hädrich S, Seise E et al. Fiber-amplifier pumped high average power few-cycle pulse non-collinear OPCPA. *Opt Express* **18**, 4689–4694 (2010).
95. Rothhardt J, Hädrich S, Seise E, Krebs M, Tavella F et al. High average and peak power few-cycle laser pulses delivered by fiber pumped OPCPA system. *Opt Express* **18**, 12719–12726 (2010).
96. Hädrich S, Demmler S, Rothhardt J, Jocher C, Limpert J et al. High-repetition-rate sub-5-fs pulses with 12 GW peak power from fiber-amplifier-pumped optical parametric chirped-pulse amplification. *Opt Lett* **36**, 313–315 (2011).
97. Rothhardt J, Demmler S, Hädrich S, Limpert J, Tünnermann A. Octave-spanning OPCPA system delivering CEP-stable few-cycle pulses and 22 W of average power at 1 MHz repetition rate. *Opt Express* **20**, 10870–10878 (2012).
98. Schultze M, Binhammer T, Steinmann A, Palmer G, Emons M et al. Few-cycle OPCPA system at 143 kHz with more than 1 μ J of pulse energy. *Opt Express* **18**, 2836–2841 (2010).
99. Schultze M, Binhammer T, Palmer G, Emons M, Lang T et al. Multi- μ J, CEP-stabilized, two-cycle pulses from an OPCPA system with up to 500 kHz repetition rate. *Opt Express* **18**, 27291–27297 (2010).
100. Herrmann D, Homann C, Tautz R, Scharrer M, Russell PSJ et al. Approaching the full octave: noncollinear optical parametric chirped pulse amplification with two-color pumping. *Opt Express* **18**, 18752–18762 (2010).
101. Harth A, Schultze M, Lang T, Binhammer T, Rausch S et al. Two-color pumped OPCPA system emitting spectra spanning 1.5 octaves from VIS to NIR. *Opt Express* **20**, 3076–3081 (2012).
102. Ahrens J, Prochnow O, Binhammer T, Lang T, Schulz B et al. Multipass OPCPA system at 100 kHz pumped by a CPA-free solid-state amplifier. *Opt Express* **24**, 8074–8080 (2016).
103. Matyschok J, Lang T, Binhammer T, Prochnow O, Rausch S et al. Temporal and spatial effects inside a compact and CEP stabilized, few-cycle OPCPA system at high repetition rates. *Opt Express* **21**, 29656–29665 (2013).
104. Harth A, Guo C, Cheng YC, Losquin A, Miranda M et al. Compact 200 kHz HHG source driven by a few-cycle OPCPA. *J Opt* **20**, 014007 (2018).
105. Prinz S, Häfner M, Schultze M, Teisset CY, Bessing R et al. Active pump-seed-pulse synchronization for OPCPA with sub-2-fs residual timing jitter. *Opt Express* **22**, 31050–31056 (2014).
106. Prinz S, Häfner M, Teisset CY, Bessing R, Michel K et al. CEP-stable, sub-6 fs, 300-kHz OPCPA system with more than

- 15 W of average power. *Opt Express* **23**, 1388–1394 (2015).
107. Hrisafov S, Pupeikis J, Chevreuil PA, Brunner F, Phillips CR et al. High-power few-cycle near-infrared OPCPA for soft X-ray generation at 100 kHz. *Opt Express* **28**, 40145–40154 (2020).
108. Furch FJ, Witting T, Giree A, Luan C, Schell F et al. CEP-stable few-cycle pulses with more than 190 μJ of energy at 100 kHz from a noncollinear optical parametric amplifier. *Opt Lett* **42**, 2495–2498 (2017).
109. Witting T, Furch FJ, Vrakking MJJ. Spatio-temporal characterisation of a 100 kHz 24 W sub-3-cycle NOPCPA laser system. *J Opt* **20**, 044003 (2018).
110. Lu CH, Witting T, Husakou A, Vrakking MJJ, Kung AH et al. Sub-4 fs laser pulses at high average power and high repetition rate from an all-solid-state setup. *Opt Express* **26**, 8941–8956 (2018).
111. Riedel R, Schulz M, Prandolini MJ, Hage A, Höppner H et al. Long-term stabilization of high power optical parametric chirped-pulse amplifiers. *Opt Express* **21**, 28987–28999 (2013).
112. Höppner H, Hage A, Tanikawa T, Schulz M, Riedel R et al. An optical parametric chirped-pulse amplifier for seeding high repetition rate free-electron lasers. *New J Phys* **17**, 053020 (2015).
113. Puppini M, Deng YP, Prochnow O, Ahrens J, Binhammer T et al. 500 kHz OPCPA delivering tunable sub-20 fs pulses with 15 W average power based on an all-ytterbium laser. *Opt Express* **23**, 1491–1497 (2015).
114. Mecseki K, Windeler MKR, Miahnahri A, Robinson JS, Fraser JM et al. High average power 88 W OPCPA system for high-repetition-rate experiments at the LCLS x-ray free-electron laser. *Opt Lett* **44**, 1257–1260 (2019).
115. Riedel R, Stephanides A, Prandolini MJ, Gronloh B, Jungbluth B et al. Power scaling of supercontinuum seeded megahertz-repetition rate optical parametric chirped pulse amplifiers. *Opt Lett* **39**, 1422–1424 (2014).
116. Indra L, Batysta F, Hřibek P, Novák J, Hubka Z et al. Picosecond pulse generated supercontinuum as a stable seed for OPCPA. *Opt Lett* **42**, 843–846 (2017).
117. Mackonis P, Rodin AM. OPCPA investigation with control over the temporal shape of 1.2 ps pump pulses. *Opt Express* **28**, 12020–12027 (2020).
118. Ishii N, Kaneshima K, Kitano K, Kanai T, Watanabe S et al. Sub-two-cycle, carrier-envelope phase-stable, intense optical pulses at 1.6 μm from a BiB_3O_6 optical parametric chirped-pulse amplifier. *Opt Lett* **37**, 4182–4184 (2012).
119. Ishii N, Kaneshima K, Kanai T, Watanabe S, Itatani J. Generation of ultrashort intense optical pulses at 1.6 μm from a bismuth triborate-based optical parametric chirped pulse amplifier with carrier-envelope phase stabilization. *J Opt* **17**, 094001 (2015).
120. Yin YC, Li J, Ren XM, Zhao K, Wu Y et al. High-efficiency optical parametric chirped-pulse amplifier in BiB_3O_6 for generation of 3 mJ, two-cycle, carrier-envelope-phase-stable pulses at 1.7 μm . *Opt Lett* **41**, 1142–1145 (2016).
121. Fuji T, Ishii N, Teisset CY, Gu X, Metzger T et al. Parametric amplification of few-cycle carrier-envelope phase-stable pulses at 2.1 μm . *Opt Lett* **31**, 1103–1105 (2006).
122. Gu X, Marcus G, Deng YP, Metzger T, Teisset C et al. Generation of carrier-envelope-phase-stable 2-cycle 740- μJ pulses at 2.1- μm carrier wavelength. *Opt Express* **17**, 62–69 (2009).
123. Moses J, Huang SW, Hong KH, Mücke OD, Falcão-Filho EL et al. Highly stable ultrabroadband mid-IR optical parametric chirped-pulse amplifier optimized for superfluorescence suppression. *Opt Lett* **34**, 1639–1641 (2009).
124. Hong KH, Huang SW, Moses J, Fu X, Lai CJ et al. High-energy, phase-stable, ultrabroadband kHz OPCPA at 2.1 μm pumped by a picosecond cryogenic Yb: YAG laser. *Opt Express* **19**, 15538–15548 (2011).
125. Hong KH, Lai CJ, Siqueira JP, Krogen P, Moses J et al. Multi-mJ, kHz, 2.1 μm optical parametric chirped-pulse amplifier and high-flux soft x-ray high-harmonic generation. *Opt Lett* **39**, 3145–3148 (2014).
126. Deng YP, Schwarz A, Fattahi H, Ueffing M, Gu X et al. Carrier-envelope-phase-stable, 1.2 mJ, 1.5 cycle laser pulses at 2.1 μm . *Opt Lett* **37**, 4973–4975 (2012).
127. Marcinkevičiūtė A, Michailovas K, Butkus R. Generation and parametric amplification of broadband chirped pulses in the near-infrared. *Opt Commun* **415**, 70–73 (2018).
128. Feng TL, Heilmann A, Bock M, Ehrentraut L, Witting T et al. 27 W 2.1 μm OPCPA system for coherent soft X-ray generation operating at 10 kHz. *Opt Express* **28**, 8724–8733 (2020).
129. Schmidt BE, Thiré N, Boivin M, Laramée A, Poitras F et al. Frequency domain optical parametric amplification. *Nat Commun* **5**, 3643 (2014).
130. Zhang QB, Takahashi EJ, Mücke OD, Lu PX, Midorikawa K. Dual-chirped optical parametric amplification for generating few hundred mJ infrared pulses. *Opt Express* **19**, 7190–7212 (2011).
131. Fu YX, Takahashi EJ, Midorikawa K. High-energy infrared femtosecond pulses generated by dual-chirped optical parametric amplification. *Opt Lett* **40**, 5082–5085 (2015).
132. Xu L, Nishimura K, Suda A, Midorikawa K, Fu YX et al. Optimization of a multi-TW few-cycle 1.7- μm source based on Type-I BBO dual-chirped optical parametric amplification. *Opt Express* **28**, 15138–15147 (2020).
133. Fu YX, Xue B, Midorikawa K, Takahashi EJ. TW-scale mid-infrared pulses near 3.3 μm directly generated by dual-chirped optical parametric amplification. *Appl Phys Lett* **112**, 241105 (2018).
134. Neuhaus M, Fuest H, Seeger M, Schötz J, Trubetskov M et al. 10 W CEP-stable few-cycle source at 2 μm with 100 kHz repetition rate. *Opt Express* **26**, 16074–16085 (2018).
135. Pupeikis J, Chevreuil PA, Bigler N, Gallmann L, Phillips CR et al. Water window soft x-ray source enabled by a 25 W few-cycle 2.2 μm OPCPA at 100 kHz. *Optica* **7**, 168–171 (2020).
136. Bigler N, Pupeikis J, Hrisafov S, Gallmann L, Phillips CR et al. Decoupling phase-matching bandwidth and interaction geometry using non-collinear quasi-phase-matching gratings. *Opt Express* **26**, 6036–6045 (2018).
137. Bigler N, Pupeikis J, Hrisafov S, Gallmann L, Phillips CR et al. High-power OPCPA generating 1.7 cycle pulses at 2.5 μm . *Opt Express* **26**, 26750–26757 (2018).
138. Shamir Y, Rothhardt J, Hädrich S, Demmler S, Tschernajew M et al. High-average-power 2 μm few-cycle optical parametric chirped pulse amplifier at 100 kHz repetition rate. *Opt Lett* **40**, 5546–5549 (2015).
139. Rudd JV, Law RJ, Luk TS, Cameron SM. High-power optical parametric chirped-pulse amplifier system with a 1.55 μm signal and a 1.064 μm pump. *Opt Lett* **30**, 1974–1976 (2005).
140. Kraemer D, Cowan ML, Hua RZ, Franjic K, Miller RJD. High-

- power femtosecond infrared laser source based on noncollinear optical parametric chirped pulse amplification. *J Opt Soc Am B* **24**, 813–818 (2007).
141. Rotermund F, Yoon CJ, Petrov V, Noack F, Kurimura S et al. Application of periodically poled stoichiometric LiTaO₃ for efficient optical parametric chirped pulse amplification at 1 kHz. *Opt Express* **12**, 6421–6427 (2004).
 142. Rotermund F, Yoon CJ, Kim K, Lim K, Kurimura S et al. Optical parametric chirped pulse amplification of Cr: forsterite laser pulses in periodically poled stoichiometric LiTaO₃ at 1 kHz. *Appl Phys B* **85**, 17–20 (2006).
 143. Cho WB, Kim K, Lim H, Lee J, Kurimura S et al. Multikilohertz optical parametric chirped pulse amplification in periodically poled stoichiometric LiTaO₃ at 1235 nm. *Opt Lett* **32**, 2828–2830 (2007).
 144. de Faria Pinto T, Mathijssen J, Eikema KSE, Witte S. Optical parametric chirped pulse amplifier producing ultrashort 10.5 mJ pulses at 1.55 μm . *Opt Express* **27**, 29829–29837 (2019).
 145. Mücke OD, Sidorov D, Dombi P, Pugžlys A, Baltuška A et al. Scalable Yb-MOPA-driven carrier-envelope phase-stable few-cycle parametric amplifier at 1.5 μm . *Opt Lett* **34**, 118–120 (2009).
 146. Mücke OD, Sidorov D, Dombi P, Pugžlys A, Ališauskas S et al. 10-mJ optically synchronized CEP-stable chirped parametric amplifier at 1.5 μm . *Opt Spectrosc* **108**, 456–462 (2010).
 147. Mücke OD, Ališauskas S, Verhoef AJ, Pugžlys A, Baltuška A et al. Self-compression of millijoule 1.5 μm pulses. *Opt Lett* **34**, 2498–2500 (2009).
 148. Tsai CL, Tseng YH, Liang AY, Lin MW, Yang SD et al. Nonlinear compression of intense optical pulses at 1.55 μm by multiple plate continuum generation. *J Lightwave Technol* **37**, 5100–5107 (2019).
 149. Rigaud P, Van de Walle A, Hanna M, Forget N, Guichard F et al. Supercontinuum-seeded few-cycle mid-infrared OPCPA system. *Opt Express* **24**, 26494–26502 (2016).
 150. Jargot G, Daher N, Lavenue L, Delen X, Forget N et al. Self-compression in a multipass cell. *Opt Lett* **43**, 5643–5646 (2018).
 151. Mero M, Heiner Z, Petrov V, Rottke H, Branchi F et al. 43 W, 1.55 μm and 12.5 W, 3.1 μm dual-beam, sub-10 cycle, 100 kHz optical parametric chirped pulse amplifier. *Opt Lett* **43**, 5246–5249 (2018).
 152. Windeler MKR, Mecseki K, Miahnahri A, Robinson JS, Fraser JM et al. 100 W high-repetition-rate near-infrared optical parametric chirped pulse amplifier. *Opt Lett* **44**, 4287–4290 (2019).
 153. Erny C, Gallmann L, Keller U. High-repetition-rate femtosecond optical parametric chirped-pulse amplifier in the mid-infrared. *Appl Phys B* **96**, 257–269 (2009).
 154. Erny C, Heese C, Haag M, Gallmann L, Keller U. High-repetition-rate optical parametric chirped-pulse amplifier producing 1- μJ , sub-100-fs pulses in the mid-infrared. *Opt Express* **17**, 1340–1345 (2009).
 155. Chalus O, Bates PK, Smolarski M, Biegert J. Mid-IR short-pulse OPCPA with micro-joule energy at 100 kHz. *Opt Express* **17**, 3587–3594 (2009).
 156. Heese C, Phillips CR, Gallmann L, Fejer MM, Keller U. Ultrabroadband, highly flexible amplifier for ultrashort mid-infrared laser pulses based on aperiodically poled Mg: LiNbO₃. *Opt Lett* **35**, 2340–2342 (2010).
 157. Heese C, Phillips CR, Mayer BW, Gallmann L, Fejer MM et al. 75 MW few-cycle mid-infrared pulses from a collinear apodized APPLN-based OPCPA. *Opt Express* **20**, 26888–26894 (2012).
 158. Mayer BW, Phillips CR, Gallmann L, Fejer MM, Keller U. Sub-four-cycle laser pulses directly from a high-repetition-rate optical parametric chirped-pulse amplifier at 3.4 μm . *Opt Lett* **38**, 4265–4268 (2013).
 159. Phillips CR, Mayer BW, Gallmann L, Fejer MM, Keller U. Design constraints of optical parametric chirped pulse amplification based on chirped quasi-phase-matching gratings. *Opt Express* **22**, 9627–9658 (2014).
 160. Mayer BW, Phillips CR, Gallmann L, Keller U. Mid-infrared pulse generation via achromatic quasi-phase-matched OPCPA. *Opt Express* **22**, 20798–20808 (2014).
 161. Chalus O, Thai A, Bates PK, Biegert J. Six-cycle mid-infrared source with 3.8 μJ at 100 kHz. *Opt Lett* **35**, 3204–3206 (2010).
 162. Thai A, Hemmer M, Bates PK, Chalus O, Biegert J. Sub-250-mrad, passively carrier-envelope-phase-stable mid-infrared OPCPA source at high repetition rate. *Opt Lett* **36**, 3918–3920 (2011).
 163. Hemmer M, Thai A, Baudisch M, Ishizuki H, Taira T et al. 18- μJ energy, 160-kHz repetition rate, 250-MW peak power mid-IR OPCPA. *Chin Opt Lett* **11**, 013202 (2013).
 164. Baudisch M, Pires H, Ishizuki H, Taira T, Hemmer M, Biegert J. Sub-4-optical-cycle, 340 MW peak power, high stability mid-IR source at 160 kHz. *J Opt* **17**, 094002 (2015).
 165. Baudisch M, Wolter B, Pullen M, Hemmer M, Biegert J. High power multi-color OPCPA source with simultaneous femtosecond deep-UV to mid-IR outputs. *Opt Lett* **41**, 3583–3586 (2016).
 166. Elu U, Baudisch M, Pires H, Tani F, Frosz MH et al. High average power and single-cycle pulses from a mid-IR optical parametric chirped pulse amplifier. *Optica* **4**, 1024–1029 (2017).
 167. Thiré N, Maksimenka R, Kiss B, Ferchaud C, Bizouard P et al. 4-W, 100-kHz, few-cycle mid-infrared source with sub-100-mrad carrier-envelope phase noise. *Opt Express* **25**, 1505–1514 (2017).
 168. Thiré N, Maksimenka R, Kiss B, Ferchaud C, Gitzinger G et al. Highly stable, 15 W, few-cycle, 65 mrad CEP-noise mid-IR OPCPA for statistical physics. *Opt Express* **26**, 26907–26915 (2018).
 169. Kurucz M, Flender R, Haizer L, Nagymihaly RS, Cho W et al. 2.3-cycle mid-infrared pulses from hybrid thin-plate post-compression at 7 W average power. *Opt Commun* **472**, 126035 (2020).
 170. Flender R, Kurucz M, Grosz T, Borzsonyi A, Gimzevskis U et al. Dispersive mirror characterization and application for mid-infrared post-compression. *J Opt* **23**, 065501 (2021).
 171. Zou X, Li WK, Liang HK, Liu K, Qu SZ et al. 300 μJ , 3 W, few-cycle, 3 μm OPCPA based on periodically poled stoichiometric lithium tantalate crystals. *Opt Lett* **44**, 2791–2794 (2019).
 172. Zou X, Li WK, Qu SZ, Liu K, Li H et al. Flat-top pumped multimillijoule mid-infrared parametric chirped-pulse amplifier at 10 kHz repetition rate. *Laser Photon Rev* **15**, 2000292 (2021).
 173. Bridger M, Naranjo-Montoya OA, Tarasevitch A, Bovensiepen U. Towards high power broad-band OPCPA at 3000 nm. *Opt Express* **27**, 31330–31337 (2019).
 174. Andriukaitis G, Balčiūnas T, Ališauskas S, Pugžlys A, Baltuška A et al. 90 GW peak power few-cycle mid-infrared pulses from an optical parametric amplifier. *Opt Lett* **36**, 2755–2757 (2011).

175. Mitrofanov AV, Voronin AA, Sidorov-Biryukov DA, Pugžlys A, Stepanov EA et al. Mid-infrared laser filaments in the atmosphere. *Sci Rep* 5, 8368 (2015).
176. Shumakova V, Malevich P, Ališauskas S, Voronin A, Zheltikov AM et al. Multi-millijoule few-cycle mid-infrared pulses through nonlinear self-compression in bulk. *Nat Commun* 7, 12877 (2016).
177. Zhao K, Zhong HZ, Yuan P, Xie GQ, Wang J et al. Generation of 120 GW mid-infrared pulses from a widely tunable noncollinear optical parametric amplifier. *Opt Lett* 38, 2159–2161 (2013).
178. Wang PF, Li YY, Li WK, Su HP, Shao BJ et al. 2.6 mJ/100 Hz CEP-stable near-single-cycle 4 μm laser based on OPCPA and hollow-core fiber compression. *Opt Lett* 43, 2197–2200 (2018).
179. von Grafenstein L, Bock M, Ueberschaer D, Zawilski K, Schunemann P et al. 5 μm few-cycle pulses with multi-gigawatt peak power at a 1 kHz repetition rate. *Opt Lett* 42, 3796–3799 (2017).
180. Bock M, von Grafenstein L, Griebner U, Elsaesser T. Generation of millijoule few-cycle pulses at 5 μm by indirect spectral shaping of the idler in an optical parametric chirped pulse amplifier. *J Opt Soc Am B* 35, C18–C24 (2018).
181. von Grafenstein L, Bock M, Ueberschaer D, Escoto E, Koç A et al. Multi-millijoule, few-cycle 5 μm OPCPA at 1 kHz repetition rate. *Opt Lett* 45, 5998–6001 (2020).
182. Fuertjes P, von Grafenstein L, Ueberschaer D, Mei C, Griebner U et al. Compact OPCPA system seeded by a Cr: ZnS laser for generating tunable femtosecond pulses in the MWIR. *Opt Lett* 46, 1704–1707 (2021).
183. Fuertjes P, von Grafenstein L, Mei C, Bock M, Griebner U et al. Cr: ZnS-based soliton self-frequency shifted signal generation for a tunable sub-100 fs MWIR OPCPA. *Opt Express* 30, 5142–5150 (2022).
184. Sanchez D, Hemmer M, Baudisch M, Cousin SL, Zawilski K et al. 7 μm , ultrafast, sub-millijoule-level mid-infrared optical parametric chirped pulse amplifier pumped at 2 μm . *Optica* 3, 147–150 (2016).
185. Elu U, Steinle T, Sánchez D, Maidment L, Zawilski K et al. Table-top high-energy 7 μm OPCPA and 260 mJ Ho: YLF pump laser. *Opt Lett* 44, 3194–3197 (2019).
186. Voronin AA, Lanin AA, Zheltikov AM. Modeling high-peak-power few-cycle field waveform generation by optical parametric amplification in the long-wavelength infrared. *Opt Express* 24, 23207–23220 (2016).
187. Yin YC, Chew A, Ren XM, Li J, Wang Y et al. Towards terawatt sub-cycle long-wave infrared pulses via chirped optical parametric amplification and indirect pulse shaping. *Sci Rep* 7, 45794 (2017).
188. Qu SZ, Liang HK, Liu K, Zou X, Li WK et al. 9 μm few-cycle optical parametric chirped-pulse amplifier based on LiGaS₂. *Opt Lett* 44, 2422–2425 (2019).
189. Novák O, Krogen PR, Kroh T, Mocek T, Kärtner FX et al. Femtosecond 8.5 μm source based on intrapulse difference-frequency generation of 2.1 μm pulses. *Opt Lett* 43, 1335–1338 (2018).
190. Liu K, Liang HK, Li WK, Zou X, Qu SZ et al. Microjoule sub-two-cycle mid-infrared intrapulse-DFG driven by 3- μm OPCPA. *IEEE Photonics Technol Lett* 31, 1741–1744 (2019).
191. Wnuk P, Stepanenko Y, Radzewicz C. High gain broadband amplification of ultraviolet pulses in optical parametric chirped pulse amplifier. *Opt Express* 18, 7911–7916 (2010).
192. Darginavičius J, Tamošauskas G, Piskarskas A, Dubietis A. Generation of 30-fs ultraviolet pulses by four-wave optical parametric chirped pulse amplification. *Opt Express* 18, 16096–16101 (2010).
193. Mero M, Sipos A, Kurdi G, Osvay K. Generation of energetic femtosecond green pulses based on an OPCPA-SFG scheme. *Opt Express* 19, 9646–9655 (2011).
194. Pelletier E, Sell A, Leitenstorfer A, Miller RJD. Mid-infrared optical parametric amplifier based on a LGSe crystal and pumped at 1.6 μm . *Opt Express* 20, 27456–27464 (2012).
195. Valiulis G, Dubietis A, Piskarskas A. Optical parametric amplification of chirped X pulses. *Phys Rev A* 77, 043824 (2008).
196. Qian JY, Peng YJ, Li YY, Wang PF, Shao BJ et al. Femtosecond mid-IR optical vortex laser based on optical parametric chirped pulse amplification. *Photonics Res* 8, 421–425 (2020).
197. Hanna M, Druon F, Georges P. Fiber optical parametric chirped-pulse amplification in the femtosecond regime. *Opt Express* 14, 2783–2790 (2006).
198. Bigourd D, Lago L, Mussot A, Kudlinski A, Gleyze JF et al. High-gain fiber, optical-parametric, chirped-pulse amplification of femtosecond pulses at 1 μm . *Opt Lett* 35, 3480–3482 (2010).
199. Caucheteur C, Bigourd D, Hugonnot E, Szriftgiser P, Kudlinski A et al. Experimental demonstration of optical parametric chirped pulse amplification in optical fiber. *Opt Lett* 35, 1786–1788 (2010).
200. Zhou Y, Li Q, Cheung KKY, Yang SG, Chui PC et al. All-fiber-based ultrashort pulse generation and chirped pulse amplification through parametric processes. *IEEE Photonics Technol Lett* 22, 1330–1332 (2010).
201. Cristofori V, Lali-Dastjerdi Z, Rishøj LS, Gallii M, Peucheret C et al. Dynamic characterization and amplification of sub-picosecond pulses in fiber optical parametric chirped pulse amplifiers. *Opt Express* 21, 26044–26051 (2013).
202. Mussot A, Kudlinski A, d'Augères PB, Hugonnot E. Amplification of ultra-short optical pulses in a two-pump fiber optical parametric chirped pulse amplifier. *Opt Express* 21, 12197–12203 (2013).
203. Bigourd D, d'Augères PB, Duberland J, Hugonnot E, Mussot A. Ultra-broadband fiber optical parametric amplifier pumped by chirped pulses. *Opt Lett* 39, 3782–3785 (2014).
204. Vanvincq O, Fourcade-Dutin C, Mussot A, Hugonnot E, Bigourd D. Ultrabroadband fiber optical parametric amplifiers pumped by chirped pulses. Part 1: analytical model. *J Opt Soc Am B* 32, 1479–1487 (2015).
205. Fourcade-Dutin C, Vanvincq O, Mussot A, Hugonnot E, Bigourd D. Ultrabroadband fiber optical parametric amplifier pumped by chirped pulses. Part 2: sub-30-fs pulse amplification at high gain. *J Opt Soc Am B* 32, 1488–1493 (2015).
206. Fu W, Wise FW. Normal-dispersion fiber optical parametric chirped-pulse amplification. *Opt Lett* 43, 5331–5334 (2018).
207. Fu W, Herda R, Wise FW. Design guidelines for normal-dispersion fiber optical parametric chirped-pulse amplifiers. *J Opt Soc Am B* 37, 1790–1805 (2020).
208. Morin P, Duberland J, d'Augères PB, Quiquempois Y, Bouwmans G et al. μJ -level Raman-assisted fiber optical parametric chirped-pulse amplification. *Opt Lett* 43, 4683–4686 (2018).
209. Buttolph ML, Sidorenko P, Schaffer CB, Wise FW. Femto-

- second optical parametric chirped-pulse amplification in bi-refrindex step-index fiber. *Opt Lett* **47**, 545–548 (2022).
210. Qin YK, Ou YH, Cromey B, Batjargal O, Barton JK et al. Watt-level all-fiber optical parametric chirped-pulse amplifier working at 1300 nm. *Opt Lett* **44**, 3422–3425 (2019).
211. Qin YK, Batjargal O, Cromey B, Kieu K. All-fiber high-power 1700 nm femtosecond laser based on optical parametric chirped-pulse amplification. *Opt Express* **28**, 2317–2325 (2020).
212. Mori Y, Kitagawa Y. Double-line terawatt OPCPA laser system for exciting beat wave oscillations. *Appl Phys B* **110**, 57–64 (2013).
213. Hong KH, Lai CJ, Gkortsas VM, Huang SW, Moses J et al. High-order harmonic generation in Xe, Kr, and Ar driven by a 2.1- μm source: high-order harmonic spectroscopy under macroscopic effects. *Phys Rev A* **86**, 043412 (2012).
214. Rothhardt J, Krebs M, Hädrich S, Demmler S, Limpert J et al. Absorption-limited and phase-matched high harmonic generation in the tight focusing regime. *New J Phys* **16**, 033022 (2014).
215. Geiseler H, Ishii N, Kaneshima K, Kitano K, Kanai T et al. High-energy half-cycle cutoffs in high harmonic and rescattered electron spectra using waveform-controlled few-cycle infrared pulses. *J Phys B At Mol Opt Phys* **47**, 204011 (2014).
216. Lai CJ, Hong KH, Siqueira JP, Krogen P, Chang CL et al. Multi-mJ mid-infrared kHz OPCPA and Yb-doped pump lasers for tabletop coherent soft x-ray generation. *J Opt* **17**, 094009 (2015).
217. Rudawski P, Harth A, Guo C, Lorek E, Miranda M et al. Carrier-envelope phase dependent high-order harmonic generation with a high-repetition rate OPCPA-system. *Eur Phys J D* **69**, 70 (2015).
218. Chevreuil PA, Brunner F, Hrisafov S, Pupeikis J, Phillips CR et al. Water-window high harmonic generation with 0.8- μm and 2.2- μm OPCPAs at 100 kHz. *Opt Express* **29**, 32996–33008 (2021).
219. Krebs M, Hädrich S, Demmler S, Rothhardt J, Zair A et al. Towards isolated attosecond pulses at megahertz repetition rates. *Nat Photonics* **7**, 555–559 (2013).
220. Ren XM, Li J, Yin YC, Zhao K, Chew A et al. Attosecond light sources in the water window. *J Opt* **20**, 023001 (2018).
221. Witting T, Osolodkov M, Schell F, Morales F, Patchkovskii S et al. Generation and characterization of isolated attosecond pulses at 100 kHz repetition rate. *Optica* **9**, 145–151 (2022).
222. Osolodkov M, Furch FJ, Schell F, Šušnjar P, Cavalcante F et al. Generation and characterisation of few-pulse attosecond pulse trains at 100 kHz repetition rate. *J Phys B At Mol Opt Phys* **53**, 194003 (2020).
223. Popmintchev T, Chen MC, Popmintchev D, Arpin P, Brown S et al. Bright coherent ultrahigh harmonics in the keV X-ray regime from mid-infrared femtosecond lasers. *Science* **336**, 1287–1291 (2012).
224. Stein GJ, Keathley PD, Krogen P, Liang HK, Siqueira JP et al. Water-window soft x-ray high-harmonic generation up to the nitrogen K-edge driven by a kHz, 2.1 μm OPCPA source. *J Phys B At Mol Opt Phys* **49**, 155601 (2016).
225. Ishii N, Kaneshima K, Kanai T, Watanabe S, Itatani J. Generation of sub-two-cycle millijoule infrared pulses in an optical parametric chirped-pulse amplifier and their application to soft x-ray absorption spectroscopy with high-flux high harmonics. *J Opt* **20** 014003 (2018).
226. Popmintchev D, Galloway BR, Chen MC, Dollar F, Mancuso CA et al. Near- and extended-edge X-ray-absorption fine-structure spectroscopy using ultrafast coherent high-order harmonic supercontinua. *Phys Rev Lett* **120**, 093002 (2018).
227. Hoff D, Furch FJ, Witting T, Rühle K, Adolph D et al. Continuous every-single-shot carrier-envelope phase measurement and control at 100 kHz. *Opt Lett* **43**, 3850–3853 (2018).
228. Mitrofanov AV, Sidorov-Biryukov DA, Rozhko MV, Ryabchuk SV, Voronin AA et al. High-order harmonic generation from a solid-surface plasma by relativistic-intensity sub-100-fs mid-infrared pulses. *Opt Lett* **43**, 5571–5574 (2018).
229. Weisshaupt J, Juvé V, Holtz M, Ku S, Woerner M et al. High-brightness table-top hard X-ray source driven by sub-100-femtosecond mid-infrared pulses. *Nat Photonics* **8**, 927–930 (2014).
230. Puppim M, Deng Y, Nicholson CW, Feldl J, Schröter NBM et al. Time- and angle-resolved photoemission spectroscopy of solids in the extreme ultraviolet at 500 kHz repetition rate. *Rev Sci Instrum* **90**, 023104 (2019).
231. Wolter B, Pullen MG, Baudisch M, Sclafani M, Hemmer M et al. Strong-field physics with mid-IR fields. *Phys Rev X* **5**, 021034 (2015).
232. Amini K, Sclafani M, Steinle T, Le AT, Sanchez A et al. Imaging the Renner-Teller effect using laser-induced electron diffraction. *Proc Natl Acad Sci USA* **116**, 8173–8177 (2019).
233. Woodbury D, Feder L, Shumakova V, Gollner C, Schwartz R et al. Laser wakefield acceleration with mid-IR laser pulses. *Opt Lett* **43**, 1131–1134 (2018).
234. Samsonova Z, Höfer S, Kaymak V, Ališauskas S, Shumakova V et al. Relativistic interaction of long-wavelength ultrashort laser pulses with nanowires. *Phys Rev X* **9**, 021029 (2019).
235. Manzoni C, Mücke OD, Cirmi G, Fang SB, Moses J et al. Coherent pulse synthesis: towards sub-cycle optical waveforms. *Laser Photon Rev* **9**, 129–171 (2015).
236. Huang SW, Cirmi G, Moses J, Hong KH, Bhardwaj S et al. High-energy pulse synthesis with sub-cycle waveform control for strong-field physics. *Nat Photonics* **5**, 475–479 (2011).
237. Çankaya H, Calendron AL, Zhou C, Chia SH, Mücke OD et al. 40- μJ passively CEP-stable seed source for ytterbium-based high-energy optical waveform synthesizers. *Opt Express* **24**, 25169–25180 (2016).
238. Muschet AA, De Andres A, Fischer P, Salh R, Veisz L. Utilizing the temporal superresolution approach in an optical parametric synthesizer to generate multi-TW sub-4-fs light pulses. *Opt Express* **30**, 4374–4380 (2022).
239. Huang SW, Cirmi G, Moses J, Hong KH, Bhardwaj S et al. Optical waveform synthesizer and its application to high-harmonic generation. *J Phys B At Mol Opt Phys* **45**, 074009 (2012).
240. Biegert J, Bates PK, Chalus O. New mid-infrared light sources. *IEEE J Sel Top Quantum Electron* **18**, 531–540 (2012).
241. Luther BM, Tracy KM, Gerrity M, Brown S, Krummel AT. 2D IR spectroscopy at 100 kHz utilizing a mid-IR OPCPA laser source. *Opt Express* **24**, 4117–4127 (2016).
242. Suchowski H, Krogen PR, Huang SW, Kärtner FX, Moses J. Octave-spanning coherent mid-IR generation via adiabatic difference frequency conversion. *Opt Express* **21**, 28892–28901 (2013).
243. Krogen P, Suchowski H, Liang HK, Flemens N, Hong KH et al. Generation and multi-octave shaping of mid-infrared intense

- single-cycle pulses. *Nat Photonics* **11**, 222–226 (2017).
244. Kartashov D, Ališauskas S, Pugžlys A, Voronin A, Zheltikov A et al. White light generation over three octaves by femto-second filament at 3.9 μm in argon. *Opt Lett* **37**, 3456–3458 (2012).
245. Mitrofanov AV, Voronin AA, Mitryukovskiy SI, Sidorov-Biryukov DA, Pugžlys A et al. Mid-infrared-to-mid-ultraviolet supercontinuum enhanced by third-to-fifteenth odd harmonics. *Opt Lett* **40**, 2068–2071 (2015).
246. Kartashov D, Ališauskas S, Pugžlys A, Voronin A, Zheltikov A et al. Mid-infrared laser filamentation in molecular gases. *Opt Lett* **38**, 3194–3197 (2013).
247. Kartashov D, Ališauskas S, Pugždzlys A, Voronin AA, Zheltikov AM et al. Third- and fifth-harmonic generation by mid-infrared ultrashort pulses: beyond the fifth-order nonlinearity. *Opt Lett* **37**, 2268–2270 (2012).
248. Kartashov D, Ališauskas S, Andriukaitis G, Pugžlys A, Shneider M et al. Free-space nitrogen gas laser driven by a femtosecond filament. *Phys Rev A* **86**, 033831 (2012).
249. Malevich PN, Maurer R, Kartashov D, Ališauskas S, Lanin AA et al. Stimulated Raman gas sensing by backward UV lasing from a femtosecond filament. *Opt Lett* **40**, 2469–2472 (2015).
250. Mitrofanov AV, Voronin AA, Sidorov-Biryukov DA, Mitryukovsky SI, Fedotov AB et al. Subterawatt few-cycle mid-infrared pulses from a single filament. *Optica* **3**, 299–302 (2016).
251. Mitrofanov AV, Voronin AA, Rozhko MV, Sidorov-Biryukov DA, Fedotov AB et al. Self-compression of high-peak-power mid-infrared pulses in anomalously dispersive air. *Optica* **4**, 1405–1408 (2017).
252. Voronin AA, Mitrofanov AV, Sidorov-Biryukov DA, Fedotov AB, Pugžlys A et al. Free-beam soliton self-compression in air. *J Opt* **20**, 025504 (2018).
253. Shumakova V, Ališauskas S, Malevich P, Voronin AA, Mitrofanov AV et al. Chirp-controlled filamentation and formation of light bullets in the mid-IR. *Opt Lett* **44**, 2173–2176 (2019).
254. Mitrofanov AV, Voronin AA, Sidorov-Biryukov DA, Rozhko MV, Stepanov EA et al. Mapping anomalous dispersion of air with ultrashort mid-infrared pulses. *Sci Rep* **7**, 2103 (2017).
255. Silva F, Austin DR, Thai A, Baudisch M, Hemmer M et al. Multi-octave supercontinuum generation from mid-infrared filamentation in a bulk crystal. *Nat Commun* **3**, 807 (2012).
256. Hemmer M, Baudisch M, Thai A, Couairon A, Biegert J. Self-compression to sub-3-cycle duration of mid-infrared optical pulses in dielectrics. *Opt Express* **21**, 28095–28102 (2013).
257. Liang HK, Krogen P, Grynko R, Novak O, Chang CL et al. Three-octave-spanning supercontinuum generation and sub-two-cycle self-compression of mid-infrared filaments in dielectrics. *Opt Lett* **40**, 1069–1072 (2015).
258. Hudson DD, Baudisch M, Werdehausen D, Eggleton BJ, Biegert J. 1.9 octave supercontinuum generation in a As_2S_3 step-index fiber driven by mid-IR OPCPA. *Opt Lett* **39**, 5752–5755 (2014).
259. Zheltikov A. Multioctave supercontinua and subcycle light-wave electronics [Invited]. *J Opt Soc Am B* **36**, A168–A181 (2019).
260. Elu U, Maidment L, Vamos L, Tani F, Novoa D et al. Seven-octave high-brightness and carrier-envelope-phase-stable light source. *Nat Photonics* **15**, 277–280 (2021).
261. Mitrofanov AV, Sidorov-Biryukov DA, Nazarov MM, Voronin AA, Rozhko MV et al. Ultraviolet-to-millimeter-band supercontinua driven by ultrashort mid-infrared laser pulses. *Optica* **7**, 15–19 (2020).
262. Koulouklidis AD, Gollner C, Shumakova V, Fedorov VY, Pugžlys A et al. Observation of extremely efficient terahertz generation from mid-infrared two-color laser filaments. *Nat Commun* **11**, 292 (2020).
263. Gollner C, Shalaby M, Brodeur C, Astrauskas I, Jutas R et al. Highly efficient THz generation by optical rectification of mid-IR pulses in DAST. *APL Photonics* **6**, 046105 (2021).
264. Jovanovic I, Brown C, Wattellier B, Nielsen N, Molander W et al. Precision short-pulse damage test station utilizing optical parametric chirped-pulse amplification. *Rev Sci Instrum* **75**, 5193–5202 (2004).
265. Clady R, Coustillier G, Gastaud M, Sentis M, Spiga P et al. Architecture of a blue high contrast multiterawatt ultrashort laser. *Appl Phys B* **82**, 347–358 (2006).

Acknowledgements

We are grateful to Dr. D. Kaškelytė for building a comprehensive literature database on OPCPA. We also would like to add the following dedication at the very end of the paper: This article is dedicated to the memory of Professor Algis Petras Piskarskas (1942–2022).

Author contributions

A. Dubietis and A. Matijošius both contributed equally to this review.

Competing interests

The authors declare no competing financial interests.